ELUCIDATING THE MECHANISM OF SUBLETHAL THEAFLAVIN-3,3′-DIGALLATE (TF3)-FARNESOL COMBINATION AGAINST *STREPTOCOCCUS MUTANS*

BY

MUHAMMAD RIZWAN SHAH BIN ABDULLAH

INTERNATIONAL ISLAMIC UNIVERSITY MALAYSIA

2026

ELUCIDATING THE MECHANISM OF SUBLETHAL THEAFLAVIN-3,3′-DIGALLATE (TF3)-FARNESOL COMBINATION AGAINST *STREPTOCOCCUS MUTANS*

BY

MUHAMMAD RIZWAN SHAH BIN ABDULLAH

A dissertation submitted in fulfillment of the requirement for the degree of Master of Dental Sciences.

Kulliyyah of Dentistry
International Islamic University Malaysia

APRIL 2026

ABSTRACT

Streptococcus mutans is a key etiological agent of dental caries due to its acid tolerance, biofilm formation, and quorum sensing. Natural-derived bioactive compounds, such as theaflavin-3,3′-digallate (TF3) and farnesol (F), were investigated as safer and promising alternatives to conventional anti-cariogenic agents. This study evaluated the antibacterial activities of TF3 and F, individually and in combination (1:1), focusing on their effects on bacterial growth, biofilm formation and membrane integrity of *S. mutans*, together with an *in silico* analysis of their interactions with quorum sensing associated proteins. Minimum inhibitory concentration (MIC), minimum bactericidal concentration (MBC), and fractional inhibitory concentration (FIC) assays were performed for F, TF3, and their combination (TF3-F). Time-kill assays were conducted over six hours at 1×MIC and 2×MIC of F and TF3-F. Membrane integrity was evaluated using nucleic acid and protein leakage assays, along with crystal violet uptake analysis, followed by assessment of biofilm inhibition using a crystal violet (CV) assay at ½×MIC and ¼×MIC of F and TF3-F. Field Emission Scanning Electron Microscopy (FESEM) analysis was performed to examine the morphological changes of *S. mutans* at ½×MIC and ¼×MIC of F and TF3-F. Molecular docking was performed using PyRx to evaluate F and TF3 interaction with quorum sensing-associated proteins, with binding energy and hydrogen bond interactions analysed using BIOVIA Discovery Studio. F exhibited MIC and MBC values of 31.25 µg/mL, whereas TF3 showed no inhibitory activity up to 1000 µg/mL. The MIC and MBC for the TF3-F were 62.5 µg/mL and 125 µg/mL, respectively. However, the classification of TF3-F interaction was not determined, as TF3 alone did not exhibit a measurable MIC. In the time-kill assay, all treatments showed growth reduction up to four hours. However, regrowth was observed at six hours for ½×MIC and ¼×MIC of TF3-F, indicating bacteriostatic activities. Biofilm inhibition was highest for ½×MIC TF3-F, followed by ¼×MIC TF3-F, ½×MIC F, and ¼×MIC F. The TF3-F combination significantly disrupted membrane integrity, indicated by an increase in OD260/280 readings and crystal violet uptake. FESEM results provided visual confirmation that the ½×MIC TF3-F, and ¼×MIC TF3-F severely disrupted *S. mutans* morphology and membrane integrity, exceeding the effects of F alone. Molecular docking revealed that TF3 exhibited the lowest free binding energies and highest number of hydrogen bond interactions with targeted active residues, suggesting that TF3 potentially inhibit the quorum sensing of *S. mutans*. Overall, the TF3-F combination demonstrated multi-targeted antibacterial activities against *S. mutans*, encompassing biofilm suppression, membrane disruption, and potential interference with quorum sensing pathways.

ملخص البحث

تُعَدّ العقدية الطافرة (*Streptococcus mutans*) عامل مسبب رئيسي لتسوس الأسنان نظرًا لقدرتها على مقاومة الأحماض، وتكوين البيوفيلم وتفعيل آليات الإستشعار النصابي. تم فحص المركبات النشطة بيولوجيًا المشتقة من الطبيعة، الثيافلافين-3،3'-ديغالات (TF3) والفارنيسول (F)، كبدائل أكثر أمانًا وواعدة للعوامل التقليدية المضادة للتسوس. تقوم هذه الدراسة بتقييم الأنشطة المضادة للبكتيريا لـ TF3 و F، بشكل فردي ومجتمع (1:1)، مع التركيز على تأثيراتها على نمو البكتيريا وتكوين الأغشية الحيوية وسلامة غشاء *S. mutans*، بالإضافة إلى تحليل حاسوبي لتفاعلاتها مع البروتينات المرتبطة باستشعار النصاب. لهذا تم إجراء إختبارات الحدّ الأدنى للتركيز المثبط (MIC)، والحدّ الأدنى للتركيز القاتل للبكتيريا (MBC)، وتركيز التثبيط الكسري (FIC) لكلٍّ من الفارنيسول وTF3 ومزيجهما (TF3–F). كما أُجري إختبار القتل الزمني لمدة 6 ساعات عند تركيزي 1×MIC و2×MIC للفارنيسول وللمزيج TF3–F . تم تقييم سلامة الغشاء باستخدام فحوصات تسرب الأحماض النووية والبروتين، إلى جانب تحليل امتصاص البنفسجي البلوري، متبوعًا بتقييم تثبيط الغشاء الحيوي باستخدام فحص البنفسجي البلوري (CV) عند ½×MIC و ¼×MIC من F و TF3-F. كما إستُخدم المجهر الإلكتروني الماسح بانبعاث الحقل (FESEM) لدراسة التغيرات المورفولوجية في *S. mutans* عند تركيزي ½×MIC و¼×MIC للفارنيسول وTF3–F. وأُجري الإلتحام الجزيئي باستخدام برنامج PyRx لتقييم تفاعل الفارنيسول وTF3 مع البروتينات المرتبطة بآليات الإستشعار النصابي، بينما تم تحليل طاقات الإرتباط وتفاعلات الروابط الهيدروجينية بإستخدام برنامج BIOVIA Discovery Studio. أظهر الفارنيسول قيم MIC وMBC مقدارها 31.25 µg/mL، في حين لم يُظهر TF3 أي نشاط مثبط حتى تركيز 1000 µg/mL. أما مزيج TF3-F فقد سجّل قيم MIC وMBC مقدارها 62.5 µg/mL و125 µg/mL على التوالي. وفي إختبار القتل الزمني، أظهرت جميع المعالجات إنخفاضًا في النمو حتى الساعة الرابعة من التجربة، ثم لوحظ عودة البكتيريا للنمو عند الساعة السادسة لكلٍّ من تركيزي ½×MIC و¼×MIC لمزيج TF3–F مما أشار إلى أنشطة مثبطة لنمو البكتيريا. وكان أعلى تثبيط للبيوفيلم عند تركيز ½×MIC للمزيج TF3–F، يليه ¼×MIC للمزيج TF3–F، ثم ½×MIC للفارنيسول، و¼×MIC للفارنيسول. وقد تسبب مزيج TF3–F في تدمير غشاء الخلية، كما ظهر إرتفاع في قيم الامتصاص عند الأطوال الموجية OD260/280 وزيادة إمتصاص السائل البنفسجي البلوري. وأكدت نتائج FESEM أن تركيزي ½×MIC و¼×MIC من TF3-F سبّبا تلفًا مورفولوجيًا و نفاذية غشاء خلايا *S. mutans* مقارنة بالفارنيسول بشكل منفصل. بينما أظهر الإلتحام الجزيئي أن TF3 يتطلب طاقات الربط الحرة و أعلى عدد من للروابط الهيدروجينية مع البقايا النشطة للبروتينات المستهدفة. وبشكل عام، تبين أن مزيج TF3-F لدية آليات تثبيط متعددة ضد *S. mutans* تشمل تثبيط البيوفيلم، وإحداث إضطراب في غشاء الخلايا، وإمكانية التدخل في مسارات الإستشعار النصابي.

APPROVAL PAGE

I certify that I have supervised and read this study and that in my opinion, it conforms to acceptable standards of scholarly presentation and is fully adequate, in scope and quality, as a dissertation for the degree of Master of Dental Sciences

……..…….

Asst. Prof. Dr. Anis Fadhlina Izyani Binti Awang

Supervisor

……..…….

Prof. Ts. Dr. Mohd Hafiz Bin Arzmi

Co-Supervisor I

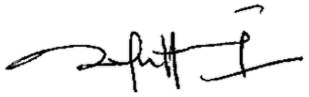

……..…….

Prof. Dr. Wan Himratul Aznita Binti Wan Harun

Co-Supervisor II

I certify that I have read this study and that in my opinion it conforms to acceptable standards of scholarly presentation and is fully adequate, in scope and quality, as a dissertation for the degree of Master of Dental Sciences

…….

Assoc. Prof. Dr. Hairul Aini Binti Hamzah

Internal Examiner

……..

Dr Norzawani Binti Jaffar

External Examiner

This dissertation was submitted to the Department of Fundamental Dental and Medical Sciences and is accepted as a fulfilment of the requirement for the degree of Master of Dental Sciences

……
Assoc. Prof. Dr. Basma Ezzat Mustafa
Head, Department of Fundamental Dental & Medical Sciences

This dissertation was submitted to the Kulliyyah of Dentistry and is accepted as a fulfillment of the requirement for the degree of Master of Dental Sciences

...……..……
Capt. (R) Assoc. Prof. Dr. Mohd Haikal bin Muhamad Halil

Dean, Kulliyyah of Dentistry

DECLARATION

I hereby declare that this dissertation is the result of my own investigations, except where otherwise stated. I also declare that it has not been previously or concurrently submitted as a whole for any other degrees at IIUM or other institutions.

Muhammad Rizwan Shah bin Abdullah

Signature……  …… Date…15 April 2026……

INTERNATIONAL ISLAMIC UNIVERSITY MALAYSIA

DECLARATION OF COPYRIGHT AND AFFIRMATION OF FAIR USE OF UNPUBLISHED RESEARCH

ELUCIDATING THE MECHANISM OF SUBLETHAL THEAFLAVIN-3,3′-DIGALLATE(TF3)-FARNESOL COMBINATION AGAINST *STREPTOCOCCUS MUTANS*

I declare that the copyright holder of this thesis are jointly owned by the student and IIUM.

Copyright © 2026 Muhammad Rizwan Shah bin Abdullah and International Islamic University Malaysia. All rights reserved.

No part of this unpublished research may be reproduced, stored in a retrieval system, or transmitted, in any form or by any means, electronic, mechanical, photocopying, recording or otherwise without prior written permission of the copyright holder except as provided below

1. Any material contained in or derived from this unpublished research may only be used by others in their writing with due acknowledgement.

2. IIUM or its library will have the right to make and transmit copies (print or electronic) for institutional and academic purpose.

3. The IIUM library will have the right to make, store in a retrieval system and supply copies of this unpublished research if requested by other universities and research libraries.

By signing this form, I acknowledged that I have read and understand the IIUM Intellectual Property Right and Commercialization policy.

Affirmed by Muhammad Rizwan Shah bin Abdullah

…… 15 April 2026 ……..

Signature Date

This thesis is dedicated to my late beloved mother, Laila binti Zainal Abidin whose love and sacrifices continue to inspire me every day. May Allah bless her abundanlty and have mercy on her.

ACKNOWLEDGEMENTS

All praise is due to Allah, the Lord of the worlds. His mercy, guidance, and countless blessings have made me who I am today and have carried me to this stage of my journey. In every moment of struggle and despair, it was through turning to Him in prayer that I found strength, patience, and comfort. Truly, nothing would have been possible without His will. May Allah send His blessings upon our beloved Prophet Muhammad ﷺ, the best of creation, whose life and teachings continue to guide me towards perseverance, humility, and sincerity.

I would like to take this opportunity to extend my sincere appreciation to my dearest family, especially my father, Abdullah bin Ismail, and my siblings, Nor Fatihah, Idris Shah and Adam Shah. The prayers and sacrifices they have made for me and love they have given me have been the foundation of my strength and the driving force that has carried me to the completion of this journey. They reminded me to hold on to faith when I felt like giving up, and their unwavering belief in me gave me the courage to continue. This achievement is as much theirs as it is mine.

I would like to thank my friends who have stood by me with their encouragement and positivity. Their support has provided me with the motivation to strive for excellence. In particular, I want to acknowledge Zahran Mara Halim, Fawwaz Adli, Farhan Jawaz, Ahmad Farhan, Nafiz Irfan, Mashitah Ghani, Aisya Madiha, Farah Syaafiah, Aini Aqilah, Eimran Hakim, Izwan Asyaraf, Affandi Idris, Luqman Raziq, Aisyah Sofea, Noh Hazrin, Faris Edruce, Dehya Al-Qalb, Fahrin Najwan, Fahim Zamani, Aizat Izzuddin, Hasif Nizam, Adeeb, Ahmad Syaafi, Dinie Haiqal, Shafiq Haiqal, Arsyam Daslam, Aiman Hakimin, Ammar Aqil, Afham Nafi, Firdaus Mokhlis, Isyraf Haidzir, Hafiz Mahabrudy, Aqiel Effat, Muhamad Farihim, Zed, Ilham Hakimi, Adil Hazim, Faris Salman, Anas Rajhan, Ilmi Hakim, Akif Syukri, Hazman Iskandar, Syahmi Nuqman, Jafni Ilyasa, Luqman Hakim, Aqil Zafri, Nurashikin, Nurul Najihah, and Dr. Azuwan for their friendship and encouragement during this journey.

I would like to extend my appreciation to my main supervisor, Asst. Prof. Dr. Anis Fadhlina Izyani binti Awang and to my co-supervisors, Prof. Dr. Mohd Hafiz bin Arzmi, Prof. Dr. Wan Himratul Aznita binti Wan Harun as well as to our collaborator of this project from UMT, Asst. Prof. Dr. Hassan Ibrahim Sheikh for their invaluable guidance, constructive feedback, and continuous encouragement. Their mentorship has not only refined my academic work but has also shaped my growth as a researcher. I would like to appreciate the staff of the Kulliyyah of Dentistry and other Kulliyyahs of the IIUM, as well as colleagues and collaborators from UMPSA for their kind assistance, technical support, and contributions to this study. Their collective efforts and generosity have played an essential role in the successful completion of this research.

TABLE OF CONTENTS

LIST OF TABLES

LIST OF FIGURES

LIST OF SYMBOLS

AA	Arachidonic Acid
ATCC	American Type Culture Collection
BHI / BHIA / BHIB	Brain Heart Infusion agar/broth
CFU/mL	Colony-forming units per millilitre
CO_2	Carbon dioxide
CV	Crystal violet
ΔG	Gibbs free binding energy
DMSO	Dimethyl sulfoxide
dH_2O	Distilled water
ECC	Early childhood caries
EPS	Extracellular polysaccharides
F	Farnesol
FIC	Fractional Inhibitory Concentration
FICI	Fractional Inhibitory Concentration Index
FESEM	Field Emission Scanning Electron Microscopy
G	Gravitational acceleration (centrifugation, × g)
HMDS	Hexamethyldisilazane
H-bond	Hydrogen bond
HSD	Honest Significant Difference test
$\log_{10}$ CFU/mL	Logarithm (base 10) of CFU per mL
MBC	Minimum Bactericidal Concentration
MIC	Minimum Inhibitory Concentration
µg/mL	Micrograms per millilitre
mg/mL	Milligrams per millilitre
mL / µL	Millilitre / microlitre
Nm	Nanometre

OD	Optical density
PBS	Phosphate-buffered saline
PDB	Protein Data Bank
QS	Quorum Sensing
Rpm	Revolutions per minute
SD / SE	Standard deviation / standard error
SEM	Scanning Electron Microscopy
TCC	Triclocarban
TCS	Triclosan
TF3	Theaflavin-3,3′-digallate
TF3-F	Combination of TF3 and Farnesol
UT	Untreated control
UV-Vis	Ultraviolet-visible spectrophotometer
v/v / w/v	Volume-to-volume / weight-to-volume ratio

CHAPTER ONE

INTRODUCTION

1.1 BACKGROUND OF THE STUDY

Early Childhood Caries (ECC) is defined by the presence of one or more decayed, missing, or filled primary tooth surfaces in a child aged 71 months or younger (Patel et al., 2025; Rusali et al., 2019). The severity of ECC is strongly linked to the role of *Streptococcus mutans*, a bacterium capable of producing acid and thriving in biofilm communities on tooth surfaces (Almoudi et al., 2021). ECC presents a major global public health challenge, particularly affecting vulnerable populations, including children from low-income families and minority communities (Adeghe, 2024). It is an aggressive form of dental decay that is not only painful and difficult to manage but also economically burdensome. Globally, ECC is recognised as a significant public health issue, with the World Health Organisation noting its prevalence as a leading cause of early childhood tooth loss. Recent meta-analysis estimates indicate that the global prevalence of ECC is approximately 49% (95% CI: 0.44–0.55), with regional variations of 34% in Central/South America, 36% in Europe, 42% in Africa, 52% in Asia-Oceania, 57% in North America, and 72% in the Middle East (Maklennan et al., 2024). In Malaysia, ECC prevalence has been reported at approximately 70%, reflecting a significant burden comparable to other high-prevalence regions in Asia-Oceania (Maklennan et al., 2024). This condition leads to serious health and developmental

problems, including premature tooth loss, malnutrition, and diminished quality of life (Rusali et al., 2019).

According to Adeghe (2024), ECC remains a critical oral health issue, particularly in disadvantaged communities across both developing and industrialised nations, where undernutrition is prevalent. Despite advances in dental education and oral hygiene awareness, dental caries continues to pose a significant public health challenge, with global studies reporting an increase in caries prevalence (Jawdekar et al., 2024). Untreated ECC has been linked to systemic health consequences, including increased susceptibility to infections, poor nutritional status, and impaired cognitive development (Pitts et al., 2017). Severe ECC cases often require hospital-based treatments under general anaesthesia, imposing a substantial economic burden on healthcare systems and families, particularly in lower-income communities (Rusali et al., 2019)

In response, the Malaysian Ministry of Health has implemented the National Oral Health Policy (NOHPoL) and the National Oral Health Plan (NOHP) 2021-2030 through its Oral Health Programme (OHP). The plan encompasses various preventive measures, such as fluoride varnish applications for toddlers, fissure sealants, and school-based fluoride mouth rinsing programmes. However, the OHP's 2021 annual report highlighted a shortfall in achieving the target of 41% of 6-year-old children free from dental caries, indicating the need for enhanced efforts to improve oral health outcomes in Malaysia. Advanced carious lesions can cause considerable pain and negatively affect the quality of life by impairing mastication, altering appearance, disrupting sleep, and impacting daily activities. Children suffering from caries are also at risk of malnutrition, stunted growth,

and weight loss, while their parents or caregivers often endure sleepless nights and financial strain (Pitts et al., 2017).

Natural compounds such as theaflavin-3,3′-digallate (TF3), mainly found in black tea, and farnesol, a sesquiterpene alcohol derived from essential oils, have demonstrated promising antimicrobial effects. TF3 has been shown to inhibit biofilm formation, acid production, and quorum sensing, while farnesol damages bacterial membranes and induces cell death (Wint et al., 2024 & Wang et al., 2024). Together, these compounds target distinct yet complementary pathways, making them a potentially effective strategy to address the challenges posed by *S. mutans* in ECC. This concept of quorum sensing inhibition (QSI) has gained attention as an alternative strategy to combat bacterial virulence without exerting selective pressure for resistance. Despite their individual efficacy, little is known about the combination effects of TF3 and farnesol, particularly at sublethal concentrations and in the context of *S. mutans* biofilm formation and quorum sensing. Investigating these sublethal concentrations is significant as they mimic real clinical settings in which agents aim to attenuate pathogenicity without causing harm to the host or disrupting the oral microbiome. This represents a critical gap in the current research.

1.2 PROBLEM STATEMENT

ECC is strongly linked to high levels of *S. mutans* within plaque-biofilms on teeth (Almoudi et al., 2021). While current dental care products have been effective in managing *S. mutans*, concerns about the safety of these common agents have emerged, with triclosan (TCS) and triclocarban (TCC) being associated with neurotoxicity and

cardiotoxicity (Alfhili et al., 2021). TCS has also been found to alter biofilm composition and enhance the prevalence of resistant *S. mutans* populations, raising concerns about its continued use in oral healthcare products (Sinicropi et al., 2022). Chlorhexidine mouthwash is reported to have adverse side effects such as extrinsic tooth staining, dysgeusia, oral mucosal irritation, and dysbiosis even at low concentrations between 0.06%-0.2% within the therapeutic range (Deus and Ouanounou, 2022). Furthermore, prolonged exposure to fluoride has raised concerns about fluorosis, and the widespread application of fluoride induces the generation of fluoride-resistant *S. mutans* (Zhang et al., 2023), highlighting the potential for reducing the long-term effectiveness of fluoride-based treatments (Vijayakumar et al., 2021). Thus, the growing issue of antimicrobial resistance further highlights the need for safer, more sustainable alternatives to conventional treatments (Sara et al., 2024).

Current antibacterial agents employed in the prevention and treatment of dental caries, such as sodium fluoride, chlorhexidine, and stannous ions (Filho et al., 2020; Anderson et al., 2020), have been effective but encountered growing concerns and challenges. Fluoride resistance in *S. mutans* strains has been documented (Vijayakumar et al., 2021), and excessive fluoride use may lead to fluorosis, restricting its broader application (Li et al., 2021). Fluoride-resistant *S. mutans* has been found to possess adaptive mechanisms such as enhanced fluoride efflux pumps, altered metabolic pathways, and genetic mutations, which enable the bacteria to tolerate fluoride exposure (Zhang et al., 2023). These adaptations compromise the effectiveness of fluoride-based interventions, particularly in populations with high fluoride exposure, raising concerns about long-term reliance on fluoride in caries prevention (Vijayakumar et al., 2021).

Additionally, the use of TCS and TCC, common antimicrobial ingredients in toothpaste (Halden et al., 2017), has raised concerns due to potential associations with neurodevelopmental impairment, metabolic disorders, and cardiotoxicity (Alfhili et al., 2021).

Similarly, while chlorhexidine (CHX) remains a widely used antimicrobial, it has been associated with significant side effects, including extrinsic tooth staining, taste disturbances (dysgeusia), oral mucosal irritation, and potential allergic reactions (Deus & Ouanounou, 2022). Prolonged CHX exposure can lead to oral microbiome disruption, reducing beneficial bacterial populations while allowing opportunistic pathogens such as *Candida albicans* to thrive, increasing the risk of oral candidiasis (Filho et al., 2020). Additionally, bacterial resistance to CHX has been observed, with some studies reporting cross-resistance to antibiotics, further complicating its long-term application in ECC prevention (Zhang et al., 2023). Consequently, there is increasing interest in exploring alternative antimicrobial agents.

TF3 and farnesol are bioactive compounds with promising antimicrobial properties, offering an alternative to conventional agents. These compounds exhibit mechanisms of action distinct from those of fluoride and chlorhexidine, particularly by targeting quorum sensing and biofilm formation (Hacioglu et al., 2024; Wang et al., 2024), both of which are critical in the pathogenicity of *S. mutans*. Despite these promising properties, the precise mechanisms by which TF3 and farnesol influence *S. mutans*'s biofilm formation at sublethal concentrations are not fully understood. This gap in the current literature is significant, as targeting these mechanisms could offer a novel

approach to curb the early stages of caries development more effectively than existing treatments.

1.3 OBJECTIVES

1.3.1 General Objectives

To investigate the multi-targeted antibacterial activities of Theaflavin-3,3'-digallate-Farnesol (TF3-F) combinations against *S. mutans*.

1.3.2 Specific Objectives

1. To determine the efficacy of Theaflavin-3,3'-digallate (TF3), Farnesol (F), and their combination in inhibiting *S. mutans's* growth.
2. To determine the effect of TF3-F combination on the membrane integrity and biofilm formation of *S. mutans* at sublethal concentrations.
3. To investigate the potential of TF3 and F in inhibiting the quorum sensing of *S. mutans*.

1.4 RESEARCH QUESTIONS

1. Do TF3, F and their combination effectively inhibit *S. mutans*'s growth?
2. Does TF3-F combination affect the membrane integrity and biofilm formation in *S. mutans* at sublethal concentrations?

3. Do TF3 and F inhibit the quorum sensing of *S. mutans*?

1.5 RESEARCH HYPOTHESES

1. The TF3-F combination can effectively inhibit *S. mutans*.
2. The TF3-F combination can affect the membrane integrity and biofilm formation of *S. mutans* at sublethal concentrations.
3. The TF3 and F can inhibit the quorum sensing of *S. mutans*.

1.6 SIGNIFICANCE OF THE STUDY

The significance of this study lies in its potential to address ECC, a public health concern which affects a significant proportion of children, particularly in underprivileged communities. Developing safer, targeted therapies using TF3 and Farnesol could significantly reduce ECC burden, improve children's oral health-related quality of life, and support the success of national oral health strategies. Understanding how these compounds influence quorum sensing and biofilm formation in *S. mutans* at sublethal concentrations could provide novel mechanisms for preventing caries, and a quantitative assessment of their efficacy is a critical step toward clinical translation.

CHAPTER TWO

LITERATURE REVIEW

2.1 EARLY CHILDHOOD CARIES (ECC) AND ITS ETIOLOGY

2.1.1 Prevalence of ECC

Early childhood caries (ECC) is a dental condition affecting children under the age of six and is defined by the presence of one or more decayed (non-cavitated or cavitated), missing (due to caries), or filled surfaces in any primary tooth of a child aged 71 months or younger (Anil & Anand, 2017). The terminology employed to describe ECC has evolved in response to a deeper understanding of its underlying causes and progression. Earlier descriptions, such as “nursing bottle caries” or “baby bottle tooth decay”, were associated with feeding practices (Dharsini et al., 2020), but these terms have since been replaced by ECC to encompass a more complex aetiology that includes microbial, dietary, and environmental contributors (Patel et al., 2025).

ECC typically initiates soon after tooth eruption and is known for its rapid progression, particularly in the absence of preventive care. It often begins in the maxillary anterior teeth and can extend to posterior teeth if left untreated, leading to long-term impacts on oral function and child development (Mazurel et al., 2025). ECC is one of the most prevalent diseases in young children and has been closely linked with the regular consumption of sugary beverages, especially those containing sucrose. Prolonged exposure to fermentable carbohydrates, such as those found in sweetened milk, juices, or formula, particularly during night-time bottle-feeding or unrestricted snacking, facilitates

acid production by cariogenic bacteria and accelerates the caries process (Patel et al., 2025; Mazurel et al., 2025)

According to recent bibliometric and epidemiological analyses, it affects approximately 560 million children globally, ranking as the 12th most common health condition in childhood (Alamoudi, 2025). Meta-analytical data demonstrate that ECC prevalence varies significantly across different world regions. For instance, pooled prevalence estimates are 34% in Central and South America, 36% in Europe, 42% in Africa, 52% in Asia-Oceania, 57% in North America, and up to 72% in the Middle East (Patel et al., 2025). These figures reflect disparities in access to dental care, public health infrastructure, and oral health education. The global variation in ECC burden is illustrated in Figure 1, which provides a visual overview of prevalence rates by country and region, highlighting areas of particular high concern.

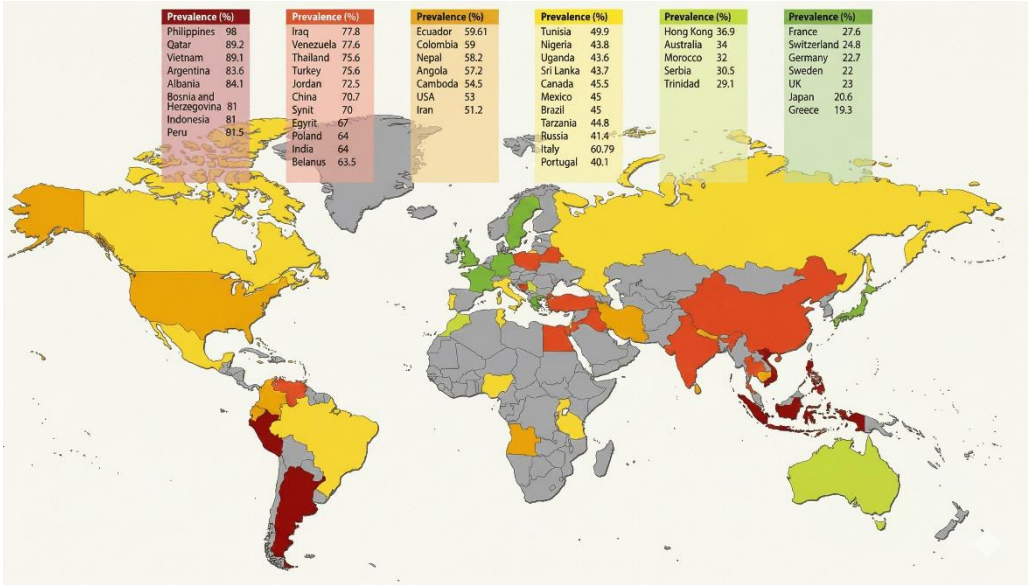

Figure 1. Worldwide ECC prevalence map. Prevalence was colour coded as follows: (a) <29%: Low prevalence (dark green), (b) 29.1-39%: Medium low prevalence (light green),

(c) 40–49.9%: Medium prevalence (yellow), (d) 50-60%: Medium high prevalence (orange), (e) 60–80%: High prevalence (light red), and (f) >80%: Very high prevalence (dark red). Source: Maklennan et al., 2024.

High prevalence rates have been particularly reported in countries within Southeast Asia. For example, national surveys have shown ECC prevalence reaching 90% among preschool children in the Philippines and Cambodia, compared to lower rates of 19-21% in countries like Japan and Greece (Patel et al., 2025). A bibliometric review of global ECC studies confirms a growing research focus on high-burden areas between 2019 and 2023, suggesting increased global recognition of the condition as a major public health concern (Alamoudi, 2025). In addition, studies investigating ECC microbiology have consistently identified *S. mutans* as a dominant organism in caries-active children, highlighting the importance of microbial ecology in ECC pathogenesis (Mazurel et al., 2025).

In Malaysia, ECC continues to be a widespread condition, particularly among children aged five and below. National oral health surveys and region-specific studies indicate that approximately 60% pre-schoolers are affected by ECC (Patel et al., 2025). These prevalence rates align with trends reported in other Southeast Asian countries. Despite the implementation of preventive programs such as the Preschool Oral Health Programme under Malaysia's Ministry of Health, ECC remains a persistent challenge, particularly in rural and underserved communities (Alamoudi, 2025). The findings from microbial studies further support the high caries risk observed in these populations, with *S. mutans* frequently detected in both saliva and plaque samples of caries-active Malaysian children (Mazurel et al., 2025). Understanding the epidemiological distribution

of ECC provides the foundation for identifying its microbial basis. Given the strong association between ECC and *S. mutans*, the next subchapter will focus on the pivotal role of *S. mutans* in ECC development.

2.1.2 Aetiology of dental caries

The development of early childhood caries (ECC) is intricately associated with the establishment and activity of cariogenic microbiota within the oral cavity such as *Streptococcus spp., Lactobacillus spp*., *Bifidobacterium*, and *Candida albicans*. Among the microbial species implicated, *S. mutans* has consistently been identified as a key etiological agent due to its acidogenicity, aciduricity, and capacity to form tenacious biofilms (Mazurel et al., 2025; Patel et al., 2025). *S. mutans* metabolises fermentable carbohydrates, particularly sucrose, into lactic acid, resulting in localised enamel demineralisation. Moreover, it synthesises extracellular polysaccharides via glucosyltransferases, which enhance its adhesion to dental surfaces and support the formation of structurally complex, acidic biofilms (Patel et al., 2025; Shamrin et al., 2025).

The pathogenesis of ECC is strongly influenced by the timing and route of *S. mutans* colonisation, which often occurs within the first two years of life. This early colonisation phase is considered a critical period in ECC development, with vertical transmission from caregivers, particularly mothers, serving as a primary mode of bacterial acquisition (Patel et al., 2025). Studies have demonstrated that elevated maternal salivary *S. mutans* levels significantly correlate with increased bacterial colonisation in their

children, suggesting that maternal microbial load is a predictive factor for early caries risk (Mazurel et al., 2025). Once *S. mutans* is established in the oral cavity, its survival is strongly favoured by frequent exposure to fermentable sugars, poor oral hygiene, and limited fluoride use, all of which are particularly prevalent in ECC-prone populations (Patel et al., 2025).

In this regard, early dietary habits have a pivotal impact not only on nutritional health but also on microbial ecology. As highlighted by Jurczak et al. (2020), early exposure to sugar-sweetened beverages (SSBs) and refined carbohydrates promotes the colonisation of *S. mutans*, predisposing children to future caries incidence. Dietary patterns formed during early childhood, especially before the age of two, are not only predictive of later eating behaviours but also influence the development of acidogenic bacterial populations. Public health guidelines from institutions like the American Heart Association and the American Academy of Paediatrics now emphasise avoiding added sugars and limiting fruit juice intake in young children to mitigate this risk.

While *S. mutans* and dietary sugars constitute pivotal determinants in the pathogenesis of ECC, ECC has been recognised to arise only when multiple factors converge (Dutta & Mohapatra, 2022). The classical concept of caries aetiology emphasises that microbial biofilms, host susceptibility, fermentable substrates, and the temporal dimension must act in concert for lesions to develop. This multifactorial framework is represented in Figure 2. Caries develops only when four critical determinants: plaque microorganisms, a susceptible host, fermentable dietary substrates, and sufficient time operate simultaneously. The absence of any single factor precludes lesion formation, underscoring the complex and conditional nature of the disease process.

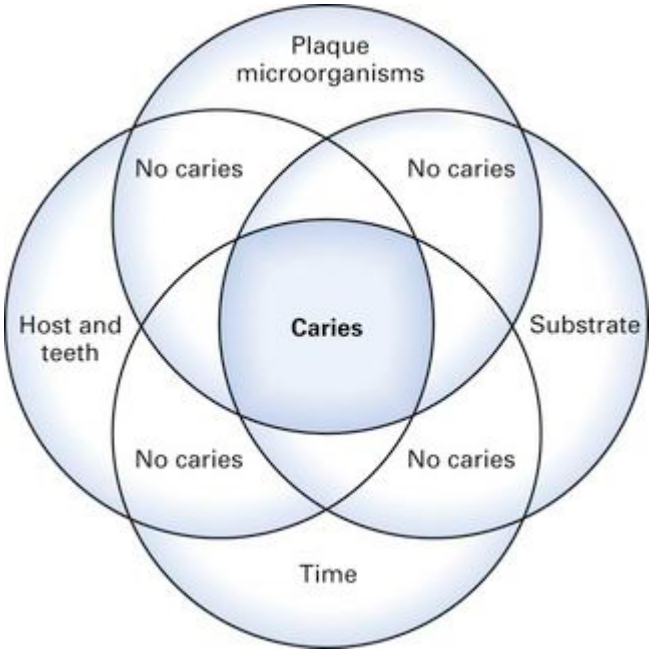

Figure 2. Multifactorial interplay in the aetiology of dental caries

2.1.3 Role of *Streptococcus mutans* in ECC development

A defining virulence trait of *S. mutans* is its ability to maintain metabolic activity and proliferation in acidic environments. This aciduric capacity enables the organism to thrive in low-pH microenvironments where other oral commensals cannot survive, effectively shifting the microbial community towards dysbiosis (Mazurel et al., 2025). The ecological plaque hypothesis aligns with this phenomenon, positing that the caries process is driven by environmental changes, particularly acidification, rather than the sole presence of specific pathogens. Despite this broader microbial context, meta-analyses confirm that *S. mutans* is consistently found at higher levels in caries-active individuals compared to caries-free controls, with both salivary and plaque samples demonstrating statistically significant differences (Mazurel et al., 2025; Shamrin et al., 2025).

Although *S. mutans* is a major contributor to ECC, it often acts in concert with other acidogenic and aciduric microorganisms. Its co-occurrence with *Lactobacillus spp*., *Bifidobacterium*, and *Candida albicans* has been frequently reported in ECC biofilms, particularly in advanced lesions (Shamrin et al., 2025; Patel et al., 2025). These microbial consortia promote a sustained low-pH environment that accelerates enamel demineralisation and lesion progression. Nevertheless, the ability of *S. mutans* to initiate early demineralisation through its unique virulence mechanisms, such as antigen I/II adhesins and acid-tolerance systems, positions it as a central driver in the initiation phase of ECC (Mazurel et al., 2025). These properties render *S. mutans* a particularly important target for microbiome-modulating preventive strategies in early childhood.

Some studies have proposed that *S. mutans* is neither universally present nor always abundant in every ECC case, raising questions about its exclusivity as a causal agent. However, the majority of high-quality evidence supports a strong association between *S. mutans* and caries presence, especially in young children with high sugar exposure and inadequate oral hygiene (Mazurel et al., 2025; Patel et al., 2025). The frequent detection of *S. mutans* in both enamel and dentin lesions, along with its known capacity to acidify and persist in the oral environment, affirms its pivotal role in caries pathogenesis. Shamrin et al. (2025) reported *S. mutans* in over 90% of various samples, reinforcing its predominance in clinical ECC cases, particularly in high-burden settings such as Southeast Asia.

2.1.4 Clinical implications of biofilm formation and acidogenicity in caries progression

The initiation and progression of early childhood caries (ECC) are closely linked to the ability of *S. mutans* to form resilient biofilms and generate acid in response to fermentable carbohydrate intake. *S. mutans* plays a central role in cariogenic biofilm formation by adhering to the tooth surface, co-aggregating with other microorganisms, and synthesising extracellular polysaccharides (EPS), which facilitate microcolony development and long-term persistence on the enamel (Patel et al., 2025; Shamrin et al., 2025). These EPS, primarily glucans produced by glucosyltransferase enzymes (Gtfs), serve as a scaffold for microbial attachment and are critical to the structural integrity and pathogenicity of dental plaque (Mazurel et al., 2025; Moon et al., 2025).

A recent finding highlights that *S. mutans* employs a two-step expansion mechanism in biofilm development: (1) Osmotic pressure-driven EPS matrix spreading, and (2) subsequent colonisation and microcolony formation on hydroxyapatite surfaces (Moon et al., 2025). This discovery challenges the classical notion of biofilm spread via bacterial motility and highlights the critical role of glucan-rich EPS in enabling the transport of bacterial clusters to new niches in the oral environment. The spread of this matrix is strongly dependent on environmental factors such as sucrose concentration and humidity, mimicking the high-sugar conditions of ECC (Moon et al., 2025).

The biofilm matrix further enhances the virulence of *S. mutans* by creating a microenvironment that favours localised acid production and retention, significantly lowering pH at the tooth-biofilm interface. The dense matrix of the biofilm impedes diffusion of acids out of the biofilm and the penetration of salivary buffers in, allowing

acids produced by *S. mutans* to remain in contact with the enamel surface, thereby initiating and sustaining demineralisation (Mazurel et al., 2025). This acidogenic behaviour is a primary factor in the pathophysiology of ECC, as sustained low pH results in the dissolution of hydroxyapatite crystals within the enamel (Patel et al., 2025; Hossain et al., 2025).

Furthermore, clinical studies confirm that *S. mutans* biofilms in caries-active individuals are denser and structurally more organised than those in caries-free subjects. The presence of *S. mutans* alongside other acidogenic species such as *Lactobacillus spp.* and *Candida albicans* forms synergistic polymicrobial communities that perpetuate acidic conditions, thus exacerbating caries severity (Patel et al., 2025). The persistence of these communities is largely attributed to the acidogenic and aciduric characteristics of *S. mutans*, which reinforce biofilm-mediated demineralisation.

In Malaysian and other Southeast Asian populations, where ECC prevalence remains high, high salivary and plaque levels of *S. mutans* have been consistently documented (Patel et al., 2025; Alamoudi, 2025). While some authors argue that *S. mutans* alone cannot explain all ECC cases, its biofilm-forming and acid-producing capabilities make it the most consistent microbial marker of caries risk (Mazurel et al., 2025; Moon et al., 2025). These findings emphasise the critical need for therapeutic strategies that target both biofilm regulation and acidogenic suppression to effectively manage and prevent ECC.

2.2 *STREPTOCOCCUS MUTANS:* VIRULENCE FACTORS & PATHOGENICITY

2.2.1 Acid production and tolerance mechanisms

S. mutans is widely recognised as a primary contributor to dental caries, particularly in early childhood caries (ECC), due to its highly specialised virulence mechanisms that enable it to produce acid (acidogenicity) and tolerate acidic (aciduricity) environments. Mechanistically, it rapidly ferments dietary carbohydrates, particularly sucrose, into lactic acid via glycolysis (Quivey et al., 2016). It utilises the phosphoenolpyruvate: sugar phosphotransferase system (PTS) for the uptake of carbohydrates, which remains highly functional even at low pH. This efficient transport system, coupled with active enzymatic pathways like glucosyltransferases (Gtfs), facilitates rapid sucrose metabolism and enhances extracellular polysaccharide production, further reinforcing the biofilm's structure and acidity (Moon et al., 2025). As a result, *S. mutans* can maintain a high rate of acidogenesis under frequent sugar exposure, which is typical in ECC-affected individuals.

Beyond its acidogenicity, *S. mutans* is notable for its aciduric properties which are defined as its capacity to survive and continue metabolic activity in highly acidic environments. This acid tolerance is achieved through several adaptive mechanisms, most notably the activity of proton-translocating F-ATPases. These membrane-bound enzymes actively extrude protons from the cytoplasm, enabling the cell to maintain pH homeostasis even when external conditions become highly acidic (Lemme et al., 2010; Baker et al., 2015). In acidic microenvironments, *S. mutans* upregulates the atp operon, enhancing F-ATPase activity to buffer cytoplasmic pH and sustain metabolic function

(Moon et al., 2025). These mechanisms allow *S. mutans* to not only survive but also dominate in mature, acidified dental biofilms, where many other species perish.

Several genes and regulatory systems underpin *S. mutans*' acid tolerance and virulence expression. The atpD gene, encoding a subunit of F-ATPase, is crucial in acid stress adaptation. Additionally, transcriptional regulators such as CcpA (catabolite control protein A) and the VicRK two-component regulatory system respond to environmental cues like carbohydrate availability and pH shifts to modulate expression of acid-resistance genes and virulence factors (Moon et al., 2025). These systems enable fine-tuned regulation of energy production, acid adaptation, and stress responses, thereby enhancing the ecological competitiveness of *S. mutans.* While the genetic and regulatory systems, such as atpD, CcpA, and VicRK, play a pivotal role in modulating acid resistance, these molecular processes operate within a broader cellular framework of acid tolerance responses.

S. mutans also produces mutacins (bacteriocin-like inhibitory peptides) that inhibit the growth of competing oral microbes, further supporting *S. mutans's* dominance in the biofilm (Kimijima et al., 2024). These peptides, along with EPS-mediated adherence and acid stress responses, reflect a sophisticated pathogenic strategy finely tuned for survival and persistence on the tooth surface. Clinical studies reinforce the relevance of these mechanisms. In ECC-active children, isolates of *S. mutans* consistently demonstrate enhanced acidogenic and aciduric traits compared to those from caries-free individuals (Moon et al., 2025). Similarly, in high-prevalence populations such as Malaysia, elevated salivary levels of *S. mutans* correlate with both caries severity and decreased microbial diversity, suggesting its role in driving acidic dysbiosis and ecological imbalance (Dinis

et al., 2022). These findings affirm that the acidogenic and aciduric capabilities of *S. mutans* are not merely adaptive traits but central to its pathogenic identity in ECC.

2.2.2 Molecular basis in adhesion and biofilm formation

The pathogenicity of *S. mutans* in early childhood caries (ECC) is closely associated with its capacity to adhere to tooth surfaces and develop structurally resilient biofilms. Adhesion is the first and essential step in the biofilm formation process, allowing *S. mutans* to colonise the enamel pellicle and resist removal by mechanical forces such as saliva flow or oral hygiene measures. This process is mediated by multiple surface adhesins, including antigen I/II (SpaP), which binds to salivary agglutinin glycoproteins, and glucan-binding proteins (Gbps), which recognise glucans synthesised by glucosyltransferase enzymes (Mazurel et al., 2025; Matias Regis et al., 2025). These interactions establish a stable attachment that sets the stage for biofilm maturation.

Following initial attachment, *S. mutans* secretes glucosyltransferases (Gtfs) specifically GtfB, GtfC, and GtfD that catalyse the synthesis of extracellular polysaccharides (EPS) from sucrose. GtfB is particularly essential for producing water-insoluble glucans that anchor bacterial cells to the tooth surface and each other, whereas GtfC generates both soluble and insoluble glucans, and GtfD mainly produces soluble glucans (Matias Regis et al., 2025; Mazurel et al., 2025). The EPS matrix serves not only as a physical scaffold but also as a protective barrier that maintains acidic microenvironments within the biofilm, enhancing the cariogenic potential of *S. mutans*.

The EPS-mediated architecture of *S. mutans* biofilms is further stabilised by glucan-binding proteins such as GbpB and GbpC. These proteins strengthen cell-to-cell cohesion, allowing for the development of dense, structured microcolonies on enamel surfaces (Patel et al., 2025; Matias Regis et al., 2025). In mixed-species biofilms, such as those involving *Candida albicans*, *S. mutans* GtfB can even bind to fungal α-mannan, further enhancing EPS synthesis and adhesion stability (Matias Regis et al., 2025; Jiang et al., 2025). This cross-kingdom interaction exemplifies the ecological adaptability of *S. mutans*, which can exploit co-aggregating organisms to fortify its biofilm matrix.

Recent investigations have shown that *S. mutans* membrane vesicles (MVs) play an emerging role in enhancing biofilm formation. These vesicles are enriched with Gtfs and can integrate into host or microbial surfaces, reinforcing the EPS network and increasing the density of biofilms, particularly in dual-species contexts (Matias Regis et al., 2025). Additionally, the LPXTG motif, a conserved peptide domain in several *S. mutans* surface proteins, facilitates sortase-mediated anchoring of adhesins to the cell wall, further enabling durable biofilm construction (Matias Regis et al., 2025). This structural anchoring is vital for maintaining functional protein expression on the bacterial surface during colonisation.

In vivo and *in vitro* studies have demonstrated that disrupting these adhesion pathways significantly impairs biofilm development and reduces cariogenicity. For instance, co-culture with *C. albicans* strains lacking V-ATPase genes (e.g., VMA3, VMA4, VMA11) leads to markedly reduced EPS synthesis and weakened dual-species biofilm structures, due to the inability of fungal hyphae to support *S. mutans* colonisation (Jiang et al., 2025). Furthermore, reduced expression of *gtf* and *gbp* genes in these

contexts confirms the importance of both interspecies interaction and intrinsic adhesin expression in maintaining biofilm integrity.

2.2.3 Quorum sensing and genetic regulation of virulence

The pathogenicity of *S. mutans* is also intricately regulated by quorum sensing (QS), a density-dependent signalling mechanism that coordinates the expression of virulence traits such as biofilm formation, bacteriocin production, acid tolerance, and competence. The primary QS circuits in *S. mutans* include the ComCDE system and the LuxS/AI-2 system, as well as global regulatory systems like VicRK and CiaRH (Rocha et al., 2020; Matias Regis et al., 2025). These pathways enable *S. mutans* to dynamically respond to environmental signals and coordinate behaviours that enhance survival and competitiveness in the oral cavity (Mazurel et al., 2025).

Figure 3 illustrates the QS regulatory in *S. mutans* by ComCDE system. It is initiated by the secretion of the ComC precursor peptide, which is processed and exported as the competence-stimulating peptide (CSP) by the ComAB transporter. Extracellular CSP activates the histidine kinase ComD, leading to phosphorylation of the response regulator ComE (Rocha et al., 2020; Jiang et al., 2025). Activated ComE upregulates early competence genes (*comAB*, *comC*, *comD*, *comE*), which drive production of mutacins, bacteriocins, and fratricide-related factors. In parallel, the alternative sigma factor (σ) activates late competence genes, including DNA uptake machinery (*comY*, *comYB*, *comEC*, *comFA*, *comGA*). These genes predominantly regulate the DNA uptake

machinery, enabling the cell to internalise DNA released from lysed neighbouring cells (Matias Regis et al., 2025).

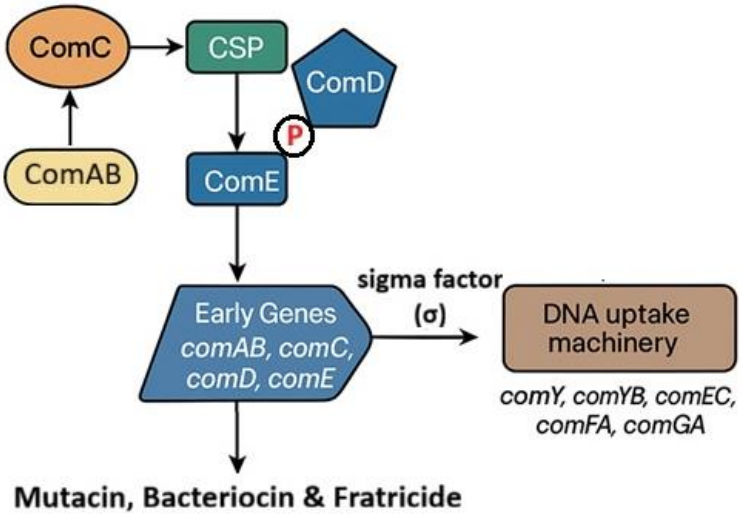

Figure 3. Quorum sensing regulatory cascade in *S. mutans* by ComCDE system

In addition to the CSP-driven peptide QS system, *S. mutans* utilises a luxS-dependent system that regulates the production of autoinducer-2 (AI-2), a signalling molecule involved in interspecies communication. LuxS activity modulates several virulence-associated pathways, including glucosyltransferase expression, exopolysaccharide synthesis, and acid tolerance (Rocha et al., 2020). Disruption of luxS has been shown to impair EPS production, alter biofilm morphology, and reduce cariogenic potential in both mono- and mixed-species models (Matias Regis et al., 2025; Jiang et al., 2025). AI-2 also influences carbohydrate metabolism and surface adhesion, indicating its broader regulatory role (Mazurel et al., 2025).

Beyond the CSP and AI-2 quorum sensing systems, *S. mutans* also employs global two-component regulatory systems such as VicRK, which respond to environmental stimuli like oxidative stress and pH changes. The VicRK system regulates expression of gtfB, gbpB, and ftf, thereby controlling EPS matrix formation, cell surface hydrophobicity, and overall biofilm stability (Rocha et al., 2020; Patel et al., 2025). Similarly, the CiaRH system contributes to stress adaptation and competence regulation, ensuring bacterial persistence under host-imposed challenges (Shamrin et al., 2025). These systems work in coordination with QS to fine-tune gene expression in response to microenvironmental cues.

Recent studies have also identified the role of RNase III family members in the post-transcriptional regulation of quorum sensing networks. Deletion of RNase III genes in *S. mutans* resulted in decreased transcription of key QS and virulence genes, including comC, gtfB, and luxS, leading to compromised biofilm structure and reduced cariogenicity in co-cultures with Candida albicans (Rocha et al., 2020; Matias Regis et al., 2025). Additionally, extracellular DNA (eDNA) within the biofilm acts as both a structural and regulatory molecule, further influencing gene regulation through feedback with QS pathways (Jiang et al., 2025).

Altogether, quorum sensing and its interconnected regulatory systems enable *S. mutans* to precisely control its virulence expression. The ComCDE and LuxS/AI-2 systems serve as core QS networks, while VicRK and RNase III contribute to environmental responsiveness and gene modulation. These mechanisms not only drive intra-species coordination but also facilitate interkingdom interactions, notably with *Candida albicans*, enhancing biofilm resilience and cariogenic potential (Matias Regis et

al., 2025; Jiang et al., 2025). Understanding these pathways provides a foundation for developing targeted anti-QS therapies derived from natural compounds that can disrupt QS-regulated gene expression and attenuate the virulence of *S. mutans*.

2.3 CURRENT ANTIMICROBIAL STRATEGIES TARGETING *S. MUTANS*

2.3.1 Conventional antimicrobial agent

The control of *S. mutans* has historically relied on conventional antimicrobial strategies. Among these, fluoride, chlorhexidine, and triclosan have been most widely used due to their proven ability to reduce microbial load, inhibit plaque formation, and suppress acidogenicity. However, recent evidence highlights that while these agents are effective under ideal conditions, their efficacy is compromised when confronting biofilm-embedded populations of *S. mutans* (Akram et al., 2025; Chen & Zhang, 2025). The intricate structure and function of biofilms create a multi-layered defence that restricts the effectiveness of conventional therapies, prompting a reassessment of their clinical applicability.

Fluoride remains the cornerstone of caries prevention due to its dual mechanism: enhancing enamel remineralisation and inhibiting demineralisation through the formation of fluoroapatite, which is more resistant to acid dissolution than hydroxyapatite (Chen & Zhang, 2025). In addition, fluoride directly interferes with microbial metabolism by inhibiting enolase and proton-extruding F1F0-ATPase, disrupting acid tolerance pathways in *S. mutans* (Akram et al., 2025). Despite this, its therapeutic effectiveness is diminished in mature biofilms, where the extracellular polymeric substance (EPS) matrix impedes fluoride ion diffusion. Furthermore, fluoride-resistant *S. mutans* subpopulations

within biofilms have been reported to exhibit tolerance levels that are several orders of magnitude higher than their planktonic counterparts (Chen & Zhang, 2025).

Chlorhexidine, a cationic bisbiguanide antiseptic, has long been utilised for its potent bactericidal activity, particularly against Gram-positive organisms such as *S. mutans*. Its mechanism of action involves binding to bacterial cell membranes, causing cytoplasmic leakage and ultimately cell death (Akram et al., 2025). Nevertheless, its clinical use is constrained by side effects, including tooth staining, altered taste sensation, mucosal desquamation, and increased supragingival calculus formation. More importantly, chlorhexidine's antimicrobial activity is significantly attenuated in the context of biofilm. Negatively charged glucans within the EPS matrix sequester the positively charged chlorhexidine molecules, impeding their penetration and reducing bactericidal efficacy (Chen & Zhang, 2025). This biofilm-mediated resistance renders chlorhexidine less effective as a monotherapy in managing ECC.

Triclosan, a synthetic phenolic compound, functions by inhibiting enoyl-acyl carrier protein reductase, thereby interfering with fatty acid synthesis in bacterial membranes. In clinical formulations such as toothpaste and mouth rinse, it has demonstrated modest reductions in plaque accumulation and gingival inflammation (Chen & Zhang, 2025). Triclosan shows moderate antimicrobial activity against *S. mutans* and inhibits its acid production. However, its utility has been questioned due to mounting concerns over endocrine-disrupting effects, environmental persistence, and the risk of antibiotic cross-resistance. Regulatory agencies in several countries have restricted or banned its use in consumer oral care products. Additionally, its non-specific mode of

action may disrupt the oral microbiome, potentially leading to dysbiosis and the proliferation of opportunistic pathogens (Akram et al., 2025).

A common challenge shared by fluoride, chlorhexidine, and triclosan is their inability to fully penetrate and eradicate biofilm-embedded *S. mutans* populations. The EPS matrix, rich in polysaccharides and extracellular DNA, acts as both a physical and biochemical barrier. This matrix not only restricts antimicrobial diffusion but also houses metabolically dormant persister cells that are inherently tolerant to antimicrobial exposure (Akram et al., 2025). Moreover, adaptive stress-response systems in *S. mutans,* such as acid tolerance response (ATR), F1F0-ATPase proton pumps, and activation of the SigX regulon, enable survival under hostile conditions, including low pH and high fluoride concentrations, further compromising the long-term efficacy of conventional treatments (Rocha et al., 2020).

2.3.2 Challenges: Antimicrobial resistance, cytotoxicity and side effects

The widespread use of fluoride, chlorhexidine, and triclosan in caries management has been pivotal in controlling *S. mutans* populations and reducing biofilm development. However, long-term reliance on these conventional agents has unveiled critical challenges, notably antimicrobial resistance, host cytotoxicity, and undesirable side effects. These concerns are particularly relevant in the context of early childhood caries (ECC), where treatment options must be both effective and biocompatible. As *S. mutans* continues to adapt within the oral environment, especially within biofilms, the clinical

utility of these agents has been called into question (Akram et al., 2025; Chen & Zhang, 2025).

Antimicrobial resistance is one of the most pressing limitations associated with conventional agents. In biofilm-associated lesions, *S. mutans* exhibits resistance mechanisms that significantly diminish the efficacy of fluoride, chlorhexidine, and triclosan. Fluoride, though effective in disrupting bacterial metabolism and promoting enamel remineralisation, shows limited penetration through the extracellular polymeric substance (EPS) matrix. Resistance within mature biofilms may be up to 1000 times greater than in planktonic cells (Chen & Zhang, 2025). Similarly, chlorhexidine's positively charged molecules are sequestered by negatively charged glucans in the EPS, preventing deep biofilm infiltration and reducing its bactericidal effect (Akram et al., 2025). Triclosan, while moderately effective, suffers from poor specificity and limited efficacy in acidic biofilm environments. These shortcomings are exacerbated by stress-response mechanisms in *S. mutans*, including the F1F0-ATPase proton pump and the SigX regulon, which enhance aciduricity and survival under chemical stress (Akram et al., 2025).

In addition to resistance, cytotoxicity is a growing concern, particularly for paediatric patients and individuals with mucosal sensitivity. Recent in vitro analyses have demonstrated that several commercially available mouthwashes containing these agents exhibit cytotoxic effects on human oral cells. Aşık et al. (2025) reported that Meridol, a fluoride-containing mouthwash, demonstrated the highest cytotoxicity on gingival fibroblasts, followed by chlorhexidine-based products such as Kloroben. These formulations significantly reduced cell viability and induced apoptosis in cultured human

cells. While antimicrobial efficacy is important, the biocompatibility of oral care products is essential for long-term use, especially in preventive strategies for children with developing oral tissues.

Chlorhexidine, although effective against Gram-positive organisms, has shown consistent drawbacks in clinical applications. Beyond its limited biofilm penetration and rising resistance, its side effects include brown staining of teeth, altered taste sensation, oral mucosal irritation, and increased supragingival calculus formation (Chen & Zhang, 2025). These effects are often dose-dependent and worsen with prolonged usage. In clinical practice, such drawbacks compromise patient compliance and may discourage routine use, particularly in young children or individuals requiring long-term prophylaxis.

Fluoride, despite its caries-preventive properties, is not without risk. When ingested excessively, especially by young children, fluoride may lead to dental fluorosis, a condition characterised by hypomineralization and enamel discolouration. In communities with high fluoride exposure, skeletal fluorosis has also been reported, although it is rare in dental contexts (Chen & Zhang, 2025). Moreover, its therapeutic impact diminishes significantly in well-established biofilms, where diffusion barriers and resistant subpopulations limit its antimicrobial reach (Akram et al., 2025).

Triclosan, once widely used in oral care products, has seen declining clinical application due to both safety concerns and ecological implications. Its non-selective antimicrobial action not only disrupts cariogenic bacteria but also affects commensal oral flora, potentially contributing to dysbiosis and the emergence of opportunistic infections. Moreover, reports of endocrine disruption and environmental accumulation have led regulatory agencies in several countries to restrict or ban triclosan in consumer products

(Chen & Zhang, 2025). These concerns further reinforce the need for targeted, selective alternatives that minimise collateral biological and environmental harm.

2.4 NATURAL ANTIMICROBIALS AS ALTERNATIVE THERAPEUTICS

2.4.1 Plant-derived antimicrobial compounds

Amidst the escalating concerns over antimicrobial resistance and the side effects associated with synthetic agents like chlorhexidine and fluoride, natural compounds have garnered substantial interest for their therapeutic potential against oral pathogens, particularly *S. mutans*. In recent years, there has been a marked surge in research and clinical interest in natural plant-derived antimicrobial agents as alternatives to synthetic therapeutics for managing oral infections, particularly dental caries. This interest is driven by rising global concerns over antimicrobial resistance and the adverse effects of conventional treatments such as chlorhexidine and fluoride. Natural compounds offer promising antimicrobial, antibiofilm, and even remineralisation properties with improved biocompatibility and fewer side effects (Chen & Zhang, 2025). Researchers are increasingly exploring phytochemicals not only for their standalone efficacy but also for their potential in synergistic combinations, reflecting a global movement toward safer, plant-based oral care solutions (Prince et al., 2022).

A wide array of plant polyphenols and flavonoids has demonstrated considerable antimicrobial action against *S. mutans*, a major contributor to dental caries. Compounds such as theaflavin, curcumin, and quercetin have attracted significant attention for their ability to suppress biofilm formation, inhibit acid production, and downregulate

virulence-associated genes (Kamarehei et al., 2022). For instance, theaflavin derived from black tea has been shown to inhibit both growth and acidogenicity of *S. mutans* and is particularly effective against mature biofilms (Chen & Zhang, 2025). Similarly, curcumin has been widely studied for its ability to reduce biofilm biomass and extracellular polysaccharide production by targeting glucosyltransferases and quorum sensing pathways, underscoring its potential as a natural antibiofilm agent (Kamarehei et al., 2022).

The exploration of synergistic plant-based combinations represents a growing frontier in natural antimicrobial research. A notable example is the synergy observed between manuka honey and cranberry extracts, specifically Types R and RE, which showed significantly enhanced antimicrobial effects against *S. mutans* compared to individual agents (Prince et al., 2022). These findings, supported by both well diffusion and checkerboard assays, highlight the value of combining phytochemicals with different mechanisms of action to enhance efficacy while minimising toxicity. The renewed interest in synergy-based approaches reflects a shift in antimicrobial strategy—moving beyond monotherapy to integrated, plant-based regimens tailored for oral pathogens.

Another indicator of increasing interest is the expanding investigation into diverse classes of natural compounds with antibiofilm activity. Research has identified flavonoids like quercetin and kaempferol, as well as phenolic acids, alkaloids, and polyphenols from grape seed, tea, and liquorice extracts, as potent disruptors of *S. mutans* biofilms (Kamarehei et al., 2022; Chen & Zhang, 2025). These compounds interfere with microbial adhesion, acidogenicity, and polysaccharide synthesis, which are the key steps in caries pathogenesis. The breadth of phytochemicals under active investigation

demonstrates the growing scientific recognition of nature's pharmacological diversity and the desire to harness it for caries prevention and oral health restoration.

Furthermore, natural antimicrobials have gained traction not only for their antimicrobial efficacy but also for their safety profiles and compatibility with long-term use. Unlike synthetic agents that may cause staining, taste alteration, or promote resistance, plant-derived agents such as epigallocatechin gallate (EGCG) and glycyrrhizin offer dual antimicrobial and antioxidant benefits with low toxicity (Chen & Zhang, 2025). This aligns with a broader public and professional preference for natural ingredients in personal care products, reinforcing the clinical relevance and acceptability of plant-derived compounds in modern dental formulations.

2.4.2 Virulence-directed therapies

The limitations of conventional antimicrobial treatments in managing persistent and biofilm-associated infections have led to growing scientific exploration of alternative, non-lethal strategies that target bacterial behaviour rather than viability. Conventional antibiotics often target planktonic cells, requiring high concentrations that not only damage host tissues but also disturb beneficial microbiota, creating selective pressure for resistance (Chen & Zhang, 2025). This has driven scientific interest toward non-lethal interventions such as targeting quorum sensing (QS) and biofilm inhibition, particularly in dental pathogens like *S. mutans*, where biofilm-associated behaviours drive cariogenicity (Kamarehei et al., 2022).

Biofilms are three-dimensional, self-produced extracellular matrices that enhance microbial survival by providing resistance to mechanical removal, antibiotics, and host immune defences. In *S. mutans*, biofilms are formed via glucosyltransferase-mediated exopolysaccharide synthesis and contribute significantly to enamel demineralisation through acid production and sustained surface colonisation (Prince et al., 2022; Kamarehei et al., 2022). Targeting biofilm development disrupts this protective architecture, impairing the ability of pathogens to maintain chronic infections. Importantly, natural compounds like theaflavin, curcumin, and grape seed procyanidins exhibit biofilm-disrupting capabilities through multiple mechanisms, such as membrane destabilisation, suppression of exopolysaccharide synthesis, and inhibition of adhesion (Chen & Zhang, 2025; Kamarehei et al., 2022).

In tandem, quorum sensing offers a promising anti-virulence target due to its central role in regulating gene expression related to biofilm maturation, acidogenesis, and stress response in *S. mutans*. By interfering with QS pathways, especially those mediated by the ComDE and LuxS systems, natural compounds can attenuate pathogenic behaviours without directly killing the cells, thereby reducing the risk of resistance development (Chen & Zhang, 2025). This is evident in studies showing that polyphenols like epigallocatechin-3-gallate (EGCG), curcumin, and theaflavin can downregulate QS-related genes, including gtfB, gtfC, and comD, leading to reduced virulence and biofilm thickness (Kamarehei et al., 2022; Chen & Zhang, 2025; Prince et al., 2022).

Unlike traditional antibiotics that often face diffusion barriers within biofilms, many natural agents remain active at sublethal levels and can penetrate the biofilm matrix. For instance, cranberry-derived proanthocyanidins combined with manuka honey

or methylglyoxal demonstrated synergistic antimicrobial effects and significantly lowered the minimum inhibitory concentration required to inhibit *S. mutans* growth and biofilm formation (Prince et al., 2022). This highlights the unique advantage of using naturally derived agents in combinations that not only suppress planktonic cells but also destabilise the communal biofilm structure and disrupt signalling molecules involved in QS regulation.

Furthermore, synthetic and semi-synthetic derivatives of natural agents have demonstrated enhanced specificity in biofilm and QS interference. Glycyrrhizin from liquorice, for instance, inhibits glucosyltransferase activity and suppresses extracellular polysaccharide formation, thereby limiting biofilm architecture and acid tolerance (Chen & Zhang, 2025). Similarly, antimicrobial peptides such as GH12 selectively target *S. mutans* virulence genes without disrupting beneficial flora, while curcumin and quercetin derivatives have been shown to reduce both adhesion and acidogenic potential without cytotoxicity (Kamarehei et al., 2022). These findings highlight the broad potential of natural antimicrobials to act as safer, resistance-mitigating agents compared to conventional antibiotics.

2.5 THEAFLAVIN-3,3'-DIGALLATE (TF3)

2.5.1 Source and chemical properties of TF3

Theaflavin-3,3′-digallate (TF3) is one of the most bioactive polyphenolic compounds found in black tea (*Camellia sinensis*), produced during the enzymatic oxidation and condensation of catechins, specifically epigallocatechin gallate (EGCG) and epicatechin

gallate (ECG), during tea fermentation. This process results in the formation of a characteristic benzotropolone ring structure, which defines theaflavins and contributes significantly to their antimicrobial properties (Wang et al., 2019). Among all theaflavin derivatives, TF3 is regarded as the most potent due to the presence of two galloyl groups, which enhance its interaction with biological targets and increase its pharmacological efficacy (Kong et al., 2021).

The chemical structure of TF3 (Figure 4) is composed of a central benzotropolone core flanked by gallate esters, making it a highly conjugated molecule with strong antioxidant potential. This configuration allows TF3 to form stable complexes with metal ions, engage in hydrogen bonding, and interact with microbial membranes and enzymes (Yi et al., 2013). The galloyl groups increase the molecule's hydrophobic and electron-rich character, which enhances its affinity for lipid bilayers and negatively charged microbial surfaces, a key property in antimicrobial function (Wang et al., 2019).

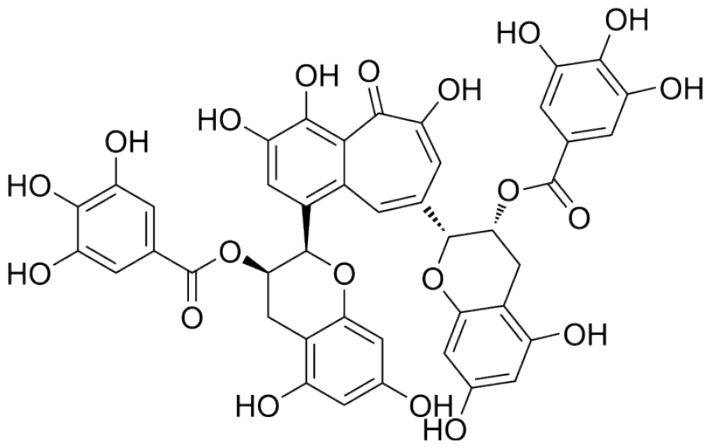

Figure 4. Chemical structure of Theaflavin-3,3′-digallate (TF3)

TF3's unique structure enables it to act as both a membrane-active agent and a modulator of microbial signalling. Its amphipathic nature permits insertion into bacterial lipid membranes, leading to destabilisation of membrane integrity and inhibition of nutrient transport systems (Yi et al., 2013). These interactions are concentration-dependent, with sublethal doses still capable of interfering with cellular communication and biofilm development in target pathogens such as *S. mutans* (Wang et al., 2019).

Additionally, TF3 exhibits excellent chemical stability in aqueous environments, maintaining its bioactivity across a wide pH range, which is crucial for its efficacy in the oral cavity, where pH fluctuations occur due to acidogenic bacterial metabolism (Kong et al., 2021). This stability ensures its compatibility for incorporation into oral healthcare formulations, such as mouthwashes or toothpaste, and supports its sustained release and prolonged antimicrobial effects against cariogenic biofilms.

Studies using proteomic and transcriptomic methods revealed that TF3 interacts with multiple bacterial targets simultaneously. It affects not only the cell wall and membrane components but also impairs essential intracellular pathways such as DNA replication and repair, protein synthesis, and metabolic regulation (Kong et al., 2021). These broad-spectrum effects are attributed to the polyphenolic nature of TF3, which allows it to disrupt protein function through oxidative stress or direct covalent modification of active sites.

Lastly, TF3’s origin from a natural dietary source emphasises its safety and low toxicity profile, which is advantageous over synthetic antimicrobial agents that often cause resistance or undesirable side effects. Its dual function, disrupting bacterial

physiology while modulating virulence, makes TF3 a promising candidate for caries prevention and other antimicrobial applications (Yi et al., 2013; Wang et al., 2019).

2.5.2 Mechanism of antimicrobial action of TF3

Theaflavin-3,3′-digallate (TF3) exerts potent antimicrobial effects by targeting multiple virulence mechanisms in *S. mutans*, particularly those involving quorum sensing and membrane integrity. TF3 has been shown to significantly downregulate two-component regulatory systems (TCSs), including VicRK, LytST, and ComDE, which are crucial for sensing environmental changes and regulating genes involved in biofilm formation, acid tolerance, and extracellular polysaccharide production (Wang et al., 2019). By interfering with these pathways, TF3 disrupts the bacterium's ability to coordinate group behaviour and maintain a cariogenic phenotype.

One of the most critical targets of TF3 is the regulation of glucosyltransferases (Gtfs: GtfB, GtfC, and GtfD), which synthesise insoluble and soluble glucans essential for biofilm matrix formation. TF3 treatment leads to the transcriptional downregulation of gtf genes, thereby reducing glucan synthesis and weakening the structural stability of the biofilm (Wang et al., 2019). In parallel, TF3 reduces the expression of glucan-binding proteins (Gbps) and other EPS-associated components, further compromising the scaffold of the biofilm (Kong et al., 2021).

TF3 also disrupts the production of extracellular DNA (eDNA), a critical element in biofilm integrity, by inhibiting *lrgA*, *lrgB*, and *srtA* genes associated with cell autolysis and membrane vesicle formation. These processes are regulated by the LytST system, and

their inhibition prevents the release of eDNA that stabilises the biofilm matrix (Wang et al., 2019). By halting these autolytic events, TF3 weakens cell-cell communication and the overall architecture of the biofilm.

In addition to targeting quorum sensing, TF3 compromises bacterial membrane integrity. Studies have shown that TF3 increases membrane permeability, leading to the leakage of intracellular contents, including nucleic acids and small molecules (Yi et al., 2013). Transmission electron microscopy (TEM) of TF3-treated cells reveals disrupted outer membranes and cytoplasmic content leakage, supporting its membrane-active mechanism. This direct damage impairs critical functions such as nutrient uptake and waste export, resulting in metabolic collapse.

TF3 also interferes with acid production and tolerance mechanisms in *S. mutans*. It inhibits the expression of key glycolytic enzymes like enolase and lactate dehydrogenase, reducing lactic acid production. Furthermore, TF3 downregulates the atpD gene involved in F-type ATPase proton transport and the aguD gene of the agmatine deiminase system, both of which contribute to intracellular pH homeostasis under acidic stress (Wang et al., 2019). This makes *S. mutans* more susceptible to acid-induced cell death, an important factor in its survival in cariogenic environments.

Collectively, TF3 employs a multifaceted mechanism of action—disrupting quorum sensing, degrading biofilm structural components, damaging bacterial membranes, and inhibiting metabolic pathways. These combined effects render *S. mutans* less virulent and less able to maintain cariogenic biofilms, positioning TF3 as a highly promising natural anti-caries agent (Kong et al., 2021; Wang et al., 2019; Yi et al., 2013).

2.6 FARNESOL

2.6.1 Source and chemical properties of farnesol

Farnesol (Figure 5) is a naturally occurring sesquiterpene alcohol found in a wide range of biological sources, including plants and fungi. It has gained notable interest due to its promising antimicrobial properties and its role in disrupting biofilm formation, particularly against oral pathogens such as *S. mutans* (Costa et al., 2025). This compound exists predominantly in the *trans, trans*-configuration (tt-farnesol), which exhibits the most potent bioactivity among its isomers (Haj-Yahya et al., 2024).

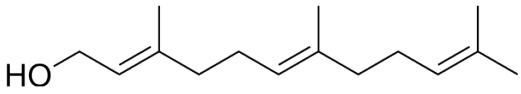

Figure 5. Chemical Structure of farnesol

As a secondary metabolite, tt-farnesol is synthesised by a variety of aromatic and medicinal plants, including chamomile, pine, citrus fruits, and also as a quorum sensing molecule by the fungal species *Candida albicans* (Haj-Yahya et al., 2024). Its biological synthesis is rooted in the mevalonate pathway, wherein farnesyl pyrophosphate (FPP) serves as a precursor. Through dephosphorylation of FPP, tt-farnesol is produced, characterised by a 15-carbon chain with three unsaturated carbon-carbon double bonds and a terminal hydroxyl group (Costa et al., 2025).

The molecular formula of tt-farnesol is $C_{15}H_{26}O$, and its structure is defined by its lipophilic nature, allowing it to integrate into lipid bilayers. This property underpins its antimicrobial efficacy by targeting bacterial membranes. The compound's hydrophobic characteristics, resulting from its long hydrocarbon chain, facilitate deep membrane penetration and potential membrane destabilisation (Kashi et al., 2025). These features are significant when assessing its pharmacodynamic behaviour and interaction with microbial cells.

Notably, tt-farnesol remains thermally stable and retains its structural integrity across a range of physiological conditions. This makes it highly suitable for incorporation into therapeutic formulations, such as dental varnishes and bioactive coatings. Its compatibility with other natural compounds, such as quercetin and theobromine, further enhances its versatility and application potential in dental care products. (Costa et al., 2025).

Furthermore, its ability to be extracted and isolated from a wide variety of botanical sources provides a sustainable and cost-effective route for pharmaceutical utilisation. Its prevalence in essential oils and propolis underscores its safety and natural integration into the human diet and oral care regimens (Haj-Yahya et al., 2024). Importantly, the U.S. Food and Drug Administration (FDA) has included farnesol on the list of substances generally recognised as safe (GRAS), further validating its therapeutic viability.

2.6.2 Mechanism of antimicrobial action of farnesol

The antimicrobial action of farnesol is multifaceted, affecting several critical physiological processes within bacterial cells. One primary mechanism is its disruption of the bacterial cell membrane. Due to its lipophilic nature, tt-farnesol integrates into phospholipid bilayers, altering membrane permeability and leading to leakage of intracellular contents. This results in cytoplasmic disorganisation and eventual cell death (Haj-Yahya et al., 2024). Flow cytometry studies using SYTO9/PI staining have confirmed increased membrane permeability upon exposure to tt-farnesol, demonstrating a significant rise in propidium iodide uptake (Haj-Yahya et al., 2024).

In addition to membrane disruption, tt-farnesol interferes with bacterial metabolic pathways. It downregulates genes involved in acid tolerance, EPS production, and glycolysis in *S. mutans*, such as *gtfB*, *gtfC*, and *gbpB* (Kashi et al., 2025). This impairs the bacterium's ability to ferment carbohydrates, produce extracellular polysaccharides, and form robust biofilms. These molecular alterations significantly reduce bacterial virulence and their cariogenic potential.

QS inhibition is another key mechanism attributed to tt-farnesol. As a known QS molecule in *C. albicans*, tt-farnesol can disrupt intercellular signalling in *S. mutans* by interfering with the expression of genes regulated by QS systems such as *comDE* and *luxS* (Costa et al., 2025; Kashi et al., 2025). These systems control biofilm formation, competence, and the regulation of virulence genes. Disrupting these signals hampers the development of mature, structured biofilms and decreases bacterial communication and resistance.

Furthermore, tt-farnesol exerts its anti-biofilm activity by affecting the structural integrity of the biofilm matrix. Scanning electron microscopy (SEM) analyses have shown that biofilms treated with tt-farnesol exhibit compromised architecture, characterised by reduced biomass, loss of extracellular matrix density, and detachment of bacterial colonies from surfaces (Costa et al., 2025). This structural disruption limits nutrient flow within the biofilm, contributing to impaired bacterial survival and colonisation.

In synergistic applications, such as its combination with arachidonic acid (AA), tt-farnesol significantly enhances antibacterial potency through additive or synergistic mechanisms. This includes reducing the MIC of AA against *S. mutans* and amplifying oxidative stress and membrane damage (Haj-Yahya et al., 2024). The combination demonstrates potential in overcoming bacterial resistance mechanisms, which is essential in managing biofilm-associated infections.

Lastly, tt-farnesol has been observed to exert a time-dependent antibacterial effect, where prolonged exposure leads to cumulative stress on bacterial cells, ultimately resulting in metabolic shutdown and cell death (Kashi et al., 2025). Unlike traditional antibiotics, tt-farnesol's natural origin and multi-targeted approach reduce the risk of resistance development.

CHAPTER 3

METHODOLOGY

3.1 PREPARATION OF COMPOUNDS

3.1.1 Amoxicillin

Amoxicillin (1g) was purchased from MedChemExpress (MCE), United States, in powder form. A stock solution of 5 mg/mL was prepared by dissolving 5.5 mg of the powder in 10% (v/v) dimethyl sulfoxide (DMSO) in distilled water (dH_2O). The use of 10% DMSO facilitated solubilisation while minimising cytotoxicity. The final concentration of the stock solution was 5 mg/mL. The solution was prepared in a sterile microcentrifuge tube, vortexed until completely dissolved, and stored at −20°C until further use.

3.1.2 Farnesol (F)

Farnesol (500 mg) was purchased from MCE in a liquid form. It (10 µL) was diluted in 990 µL of absolute ethanol to obtain a 5 mg/mL stock solution. The mixture was vortexed gently to ensure complete solubilisation. The stock solution was stored in an amber vial at −20°C to protect it from light and degradation.

3.1.3 Theaflavin-3,3′-digallate (TF3)

TF3 (10 mg) was purchased from MCE in a crystallised form. It was dissolved in 2 mL of absolute ethanol to yield a stock solution of 5 mg/mL. The solution was vortexed thoroughly until a homogeneous solution was achieved. TF3 was stored at −20°C in a light-protected container to maintain stability.

3.2 CULTIVATION OF MICROORGANISM

3.2.1 Maintenance of microorganisms

Streptococcus mutans (ATCC 25175) was purchased from the American Type Culture Collection (ATCC). The organism was cultured in brain heart infusion (BHI; Merk, Germany) broth and subsequently sub-cultured onto the BHI agar to obtain pure colonies. A long-term stock was prepared in 20% (v/v) glycerol and stored at –80°C. For routine cultivation, *S. mutans* were streaked onto BHI agar plates and incubated under microaerophilic conditions (5% CO_2) at 37°C for 24 hours.

3.2.2 Standard Curve

A standard growth curve for *S. mutans* was done to determine the growth turbidity, and cell number (CFU/mL) of the exponential phase. In order to count the colonial growth, a serial dilution was performed using normal saline as the medium of dilution. The time interval for every measurement of growth was two hours, which ended at a total period of 24 hours. For every two hours of incubation, the optical density (OD) of the inoculum was measured at 600 nm by a spectrophotometer. After the OD measurement, 100 µL of

the incubated inoculum was transferred into a tube containing 900 µL of sterile saline, which was then serially diluted by 10-fold dilution. Upon the serial dilution, 100 µL of the diluted inoculum was spread on the agar plate and incubated. The counting was done after completion of the incubation period, and a standard curve was plotted (McKernan, 2015). The density of cells at the exponential phase was determined by referring to the plotted standard curve.

3.2.3 Inoculum preparation

Single colonies were aseptically inoculated into BHI broth and cultured overnight. To obtain a standardised inoculum, the overnight culture was spectrophotometrically adjusted to an optical density (OD_{600}) of 0.07, corresponding to the early logarithmic growth phase as determined from a standard growth curve. This optical density corresponded to approximately 1×10^8 CFU/mL. This standardised inoculum was utilised in all assays. All culturing steps were conducted under sterile conditions in a Class II Biosafety Cabinet.

3.3 ANTIMICROBIAL ASSAYS

3.3.1 Minimum Inhibitory Concentration (MIC), Minimum Bactericidal Concentration (MBC) and Fractional Inhibitory Concentration (FIC) assays

The MIC and MBC of TF3, F, their combination (TF3-F), and Amoxicillin (positive control) against *S. mutans* were determined using the broth microdilution method in a 96-well plate, with adaptations from Requena et al. (2019). Freshly cultured *S. mutans*

colonies were inoculated into BHIB and incubated at 37°C in 5% CO_2 for two hours to reach the logarithmic growth phase. The bacterial suspension was then adjusted to an OD_{600} of 0.07 using fresh BHIB, corresponding to 1×10^8 CFU/mL, based on the established growth curve.

Compounds were added into the first row (well A) of the 96-well plate containing 140 µL of BHIB. The TF3 and F stock were prepared and tested in combination at a 1:1 ratio, whereby the total volume to be loaded was 40 µL (20 µL of TF3 and 20 µL of F). It was then serially diluted from well B to G vertically by two-fold with tested concentrations ranging from 1000 µg/mL to 15.6 µg/mL. Subsequently, 10 µL of the standardised inoculum was added to all wells except for the sterility controls (well H).

Wells containing only BHIB and inoculum served as the growth control, while wells containing BHIB alone were used as sterility controls. Amoxicillin was used as the positive control and tested in the same manner as the compounds, with tested concentrations ranging from 125 µg/mL to 0.98 µg/mL. Meanwhile, 40 µL of the absolute ethanol, used as the negative control, was added to 140 µL of BHIB and proceeded with a two-fold dilution. Subsequently, 10 µL of the standardised inoculum was added to all wells. The 96-well plate was then incubated at 37°C for 24 hours under 5% CO_2. Following incubation, the concentration that gave zero optical growth detected by unaided eyes was recorded as an MIC value.

To determine the MBC value, 100 µL from wells corresponding to the MIC and higher concentrations were plated on BHI agar and incubated at 37°C for 24 hours. The MBC was defined as the lowest concentration that resulted in the complete absence of

bacterial growth on agar, confirming bactericidal activity. All experiments were performed in triplicate.

The type of interactions for TF3-F was evaluated by FIC and the sum of the FIC index based on the following values: Synergy (FIC index≤0.5), additive (0.5 < FIC index≤1), indifferent (1 < FIC index≤2) and antagonism (FIC index > 2) (Haj-Yahya et al., 2024). The calculations were as follows:

- FIC of drug A = MIC of drug A in combination/MIC of drug A only
- FIC of drug B = MIC of drug B in combination/MIC of drug B only
- FIC index = FIC of drug A+FIC of drug B

3.3.2 Time-Kill Assay

The time-kill kinetics assay was conducted to evaluate the bactericidal effects of TF3-F combinations on *S. mutans* over a six-hour incubation period. This method enabled the quantitative assessment of bacterial viability following treatments (Sanguansermsri et al., 2024). *S mutans* grown to an exponential phase (1×10^8 CFU/mL) were treated with MIC and 2×MIC of F and TF3-F. For each treatment, appropriate volumes of TF3-F and F were added into 500 µL (10% of the final volume) of the adjusted bacterial suspension and topped up with BHIB to reach 5,000 µL. An untreated group containing only 500 µL of inoculum and BHIB was used as the control. All treatments were prepared in triplicate and were incubated at 37 °C. Optical density (OD) was recorded for every interval of 2, 4 and 6 hours of incubation at 600 nm. At each time interval, 100 µL of culture was also withdrawn for ten-fold serial dilutions in sterile phosphate-buffered saline (PBS).

Subsequently, 100 µL from selected ten-fold serial dilutions (10^{-2}, 10^{-4}, 10^{-6}, 10^{-8}, and 10^{-10}) were plated in duplicate onto BHI agar and incubated under the same conditions. Finally, the number of colony-forming units (CFU/mL) for each plate was enumerated.

3.3.3 Protein and Nucleic Acid Leakage Assay

To evaluate the membrane integrity of the culture upon treatment, *S. mutans* were first grown to the exponential phase (1×10^8 CFU/mL) and then diluted to an optical density (OD) of 0.07. A total of 15 Falcon tubes (15 mL capacity) were prepared for treatment, with three replicates for each experimental condition: untreated (UT), ½ MIC *TF3-F*, ¼ MIC *TF3-F*, ½ MIC *F*, and ¼ MIC *F*. Each treatment was prepared by adding the appropriate amount of bacterial inoculum and compounds to the broth. Specifically, for *TF3-F (½ MIC)*, 500 µL of inoculum was mixed with 32 µL of *TF3-F* (composed of 16 µL *F* + 16 µL *TF3*) and 4468 µL of broth. For *TF3-F (¼ MIC)*, 500 µL of inoculum was combined with 16 µL of *TF3-F* (composed of 8 µL *F* + 8 µL *TF3*) and 4484 µL of broth. For *F (½ MIC)*, 500 µL of inoculum was mixed with 16 µL of *F* and 4484 µL of broth. For *F (¼ MIC)*, 500 µL of inoculum was combined with 8 µL of *F* and 4492 µL of broth. Finally, for the untreated (UT) control, 500 µL of inoculum was mixed with 4500 µL of broth.

After preparation, the treatments were incubated at 37°C for 2 hours. Following the incubation, the cultures were centrifuged at 5000 × g for 10 minutes, and the supernatants were carefully collected. The supernatants were then analysed for the presence of nucleic acids and proteins by measuring the optical density (OD) at 260 nm

and 280 nm, respectively, using a UV-Vis spectrophotometer. The measurements were taken using quartz cuvettes to ensure accurate readings, as these cuvettes are transparent to UV light. This method allows for the evaluation of membrane integrity by quantifying nucleic acid and protein leakage, which serves as an indicator of membrane disruption due to the treatments (Moo et al., 2021).

3.3.4 Crystal Violet Uptake Assay

The crystal violet (CV) uptake assay was conducted to assess the membrane permeability of *S. mutans* following treatments (Halder et al., 2015). *S mutans* grown to an exponential phase (1×10^8 CFU/mL) were treated with ½ × MIC and ¼ × MIC of F and TF3-F. All treatments were prepared in a total volume of 5 mL and incubated at 37°C for 2 hours under 5% CO_2. Following incubation, the cultures were centrifuged at 5000 × g for 15 minutes at 4°C to pellet the cells. The harvested cell pellets were washed twice with sterile phosphate-buffered saline (PBS, pH 7.4). Each pellet was then gently resuspended in 1.5 mL of 0.01% (w/v) CV solution, freshly prepared in sterile PBS (pH 7.4), and incubated at room temperature for 30 minutes to allow the CV penetration across the membrane. After incubation, the cultures were again centrifuged under the same conditions (5000 × g, 15 minutes, 4°C), and the supernatants were carefully collected. The absorbance of the supernatant was measured at 590 nm using a spectrophotometer. The optical density reading reflects the amount of CV that remained unabsorbed in the supernatant. All experiments were performed in triplicate, with the untreated culture

serving as the control reference for baseline membrane integrity. The percentage of CV uptake was calculated using the following equation:

CV uptake (%) = [(OD 590 of control culture − OD 590 of treated culture)/OD 590 of control culture] × 100.

3.3.5 Field Emission Scanning Electron Microscopy (SEM) Analysis

Field Emission Scanning Electron Microscopy (FESEM) analysis was performed according to Murtey & Ramasamy (2021), with some modifications. *S. mutans* grown to an exponential phase (1×10^8 CFU/mL) were treated with TF3-F and F at concentrations equal to ½ × MIC value and ¼ × MIC value. All treatments were prepared in a total volume of 5 mL and incubated for 3 hours at 37 °C under 5% CO_2. After that, the cells were harvested at 5000 × g for 15 min, and the pellet was washed twice with PBS (pH 7.4). The pellet was fixed in 2.5% glutaraldehyde in PBS for 2 hours. The fixed bacterial pellet was then dehydrated in a graded alcohol series of 30%, 50%, 70%, 90%, and 100% for 20 min for each solution, with 100% dehydration conducted twice. The cells were then immersed in hexamethyldisilazane (HMDS) for two hours. The HMDS was discarded, and the pellets were dried in a desiccator overnight. Prior to the observation under FESEM, the pellet was gently crushed into powder, mounted on a carbon stub, coated with platinum using an ion sputter, and examined at 5 kV. Untreated cells were prepared in the same manner and used as a control.

3.3.6 Anti-Biofilm Assay

The anti-biofilm activity of TF3-F and F against *S. mutans* was quantitatively assessed using an anti-biofilm assay (Haj-Yahya et al., 2024). *S. mutans* grown to an exponential phase (1×10^8 CFU/mL) were treated with ½ × MIC and ¼ × MIC of F and TF3-F. All treatments were incubated in an undisturbed condition at 37°C for 24 hours under 5% CO_2 to allow for the biofilm formation. After the incubation period, the planktonic culture was carefully aspirated without disturbing the adherent biofilm. The microcentrifuge tubes were gently washed three times with PBS (pH 7.4) to remove non-adherent cells. The formed biofilms were then fixed with 1.5 mL of 99% (v/v) methanol for 15 minutes at room temperature. After the fixation step, the microcentrifuge tubes were rinsed once with PBS to eliminate residual methanol. Subsequently, the biofilms were stained with 1.5 mL of 0.1% (w/v) CV solution for 15 minutes. Excess stain was removed by washing the microcentrifuge tubes three times with distilled water, ensuring all non-specifically bound CV was eliminated. The stained biofilms were air-dried, and the bound CV was solubilised in 1.5 mL of 95% (v/v) ethanol. The optical density of the extracted CV was measured at 570 nm using a spectrophotometer to quantify the formed biofilm. All experiments were conducted in triplicate, and untreated *S. mutans* was used as a control. The percentage of biofilm inhibition was calculated using the following equation:

Biofilm inhibition (%) = [(OD 570 of control culture − OD 570 of treated culture)/OD 570 of control culture] × 100.

3.3.7 Statistical Analysis

Data was analysed using ANOVA (IBM SPSS 27.0). Results were deemed statistically significant with a p-value < 0.05 and reported as mean ± standard deviation (SD).

3.4 MOLECULAR DOCKING ANALYSIS

Molecular docking was performed to determine the binding sites and affinity of theaflavins on three main proteins (S-ribosylhomocysteinase: 4XCH; ComA: PBD 3VX4; ComE: PBD 4MLD) linked to anti-quorum sensing activities. PyRx software (version 0.8) was used for the virtual screening of the ligands and target proteins, which integrated AutoDock Vina for the molecular docking. The co-crystalised ligand was docked to its protein as a control, except for PDB 4XCH and 4MLD, as these proteins have no co-crystalised ligand bonded. The proteins and compounds were loaded as macromolecules and ligands, respectively, which were then converted into pdbqt format. The binding energy and H-bonding were used to analyse the molecular docking output. The result of all possible docked conformations of the ligands was generated and saved in an Excel file. The key parameters, such as the number of H-bonding and distance between the H-bonded residues of the proteins and ligands, were analysed by BIOVIA Discovery Studio (Fadhlina et al., 2023). The most favourable binding poses of the ligands were analysed by selecting those with the lowest free energy of binding (ΔG) and the highest number of active residues involved in the H-bonding.

3.4.1 Protein Preparation

All protein/macromolecules used were downloaded in three-dimensional (3D) structure from Protein Data Bank (https://www.rcsb.org/) as PDB files and prepared using BIOVIA Discovery Studio Visualizer. The proteins (Figure 6) were prepared by removing water molecules, adding hydrogen (polar), and defining the active site from the co-crystalised ligand prior to removing it (Fadhlina et al., 2023). The grid box (XYZ coordinates) for all proteins was determined based on their active site or around their crystal structures (Table 1). Then, the prepared proteins were saved as a pdb file.

Table 1. The coordinates of macromolecules

Macromolecules	**Classification**	**PDB ID**	**Coordinates**		
			X	**Y**	**Z**
ComA	ATP-binding cassette (ABC) transporter	3VX4	40.67	30.28	8.75
S-ribosylhomocysteinase	Lyase	4XCH	46.27	44.47	33.98
ComE	Response regulator protein	4MLD	-21.38	25.23	40.65

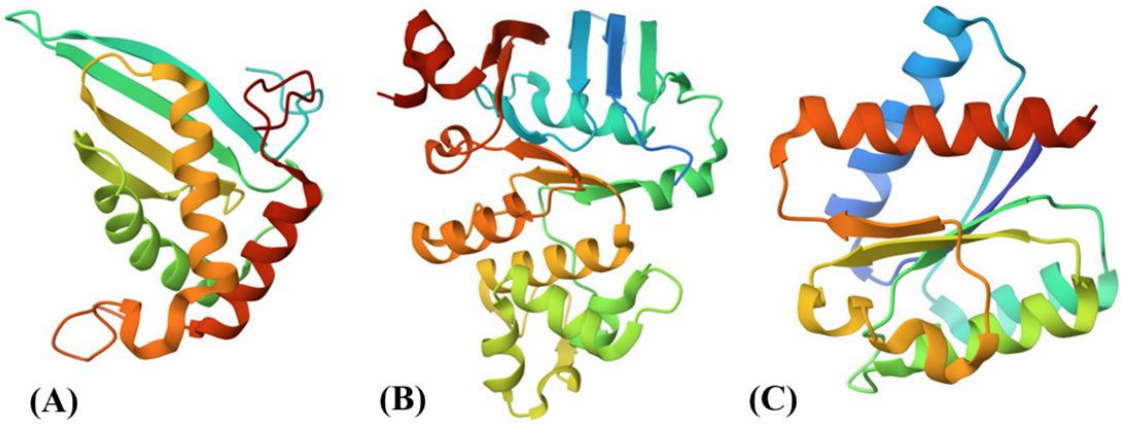

Figure 6. Quorum sensing associated proteins: (A) S-ribosylhomocysteinase; (B) ComA; (C) ComE

3.4.2 Ligand Preparation

All ligands were downloaded from PubChem library (https://pubchem.ncbi.nlm.nih.gov/) in 3D conformation as SDF file format. Avogadro software was used to prepare and optimise the ligands. The ligand preparation was done by adding hydrogen atoms and optimising the ligands' geometry until the structure became static. The prepared ligands were saved as a pdb file.

CHAPTER 4

RESULTS AND DISCUSSION

4.1 *STREPTOCOCCUS MUTANS'* GROWTH CURVE

Table 2 presents the optical density (OD_{600}) readings of *S. mutans* measured over 24 hours, while the corresponding Figure 7 illustrates its standard growth curve. The results demonstrated a typical bacterial growth pattern characterised by distinct lag, exponential, stationary, and decline phases. During the first two hours, the OD value was minimal at 0.069, representing the lag phase where cells were adapting to the new environment and synthesising essential enzymes and proteins for metabolism and replication (Choi et al., 2017). A sharp increase in OD was observed between 2 and 6 hours, reaching 2.043, marking the exponential growth phase characterized by active cell division, biomass accumulation, and high metabolic activity (Huo et al., 2011) This phase is also associated with increased carbohydrate utilization and acid production, which are key metabolic traits of *S. mutans* contributing to its cariogenic potential (Decker et al., 2014).

After six hours, the OD readings stabilised between 8 and 10 hours, indicating the stationary phase where cell growth reached equilibrium due to nutrient limitation and accumulation of metabolic by-products (Choi et al., 2017). A reduction in OD towards 24 hours suggests the decline phase, attributed to nutrient exhaustion and toxic metabolite accumulation. These results indicate that *S. mutans* exhibits rapid exponential growth within the first six hours before stabilising, emphasising that this time point represents the optimal phase for inoculum standardisation in subsequent assays.

Table 2. Growth of *S. mutans* over 24 Hours

Time (Hour)	OD Reading (OD_{600})	CFU/mL
2	0.069 ± 0.038	1.30×10^{8}
4	1.001 ± 0.534	4.10×10^{12}
6	2.043 ± 0.053	5.50×10^{12}
8	2.033 ± 0.005	1.60×10^{13}
10	2.042 ± 0.038	2.40×10^{13}
24	1.740 ± 0.159	2.57×10^{11}

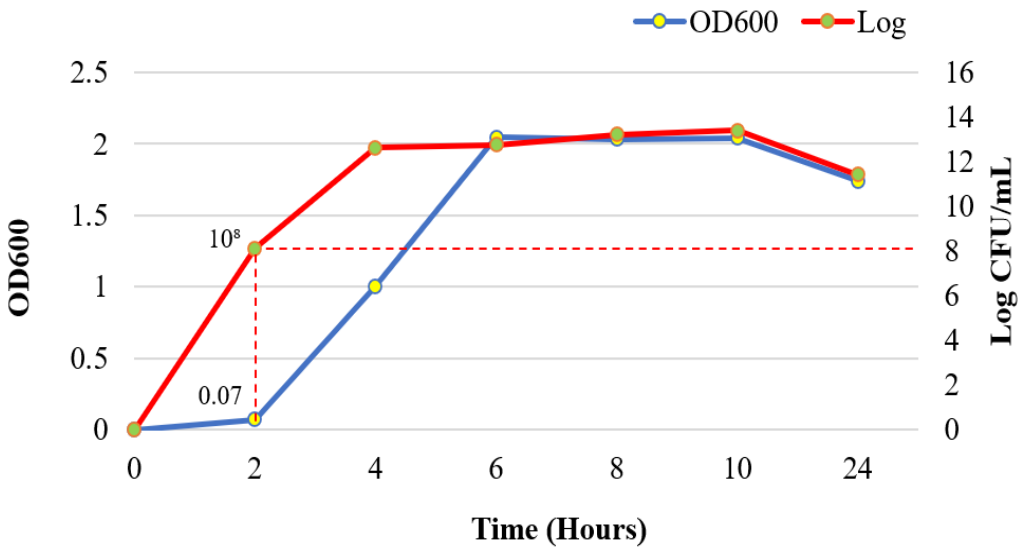

Figure 7. Growth Curve of *S. mutans* over 24 Hours

4.2 MINIMUM INHIBITORY AND BACTERICIDAL CONCENTRATION (MIC & MBC) & FRACTIONAL INHIBITORY CONCENTRATION (FIC) ASSAYS

Table 3 presents the results of the MIC, MBC and FIC assays, highlighting the antibacterial activity of individual compounds and their combination against *S. mutans*. Amoxicillin, used as a positive control, displayed potent antibacterial activity with both MIC and MBC <15.6 µg/mL, confirming the reliability of the assay results. Among the tested compounds, farnesol demonstrated the most effective antibacterial activity, with both MIC and MBC recorded at 31.25 µg/mL, indicating its bactericidal effects against *S. mutans*. In contrast, TF3 showed no detectable antibacterial activity, indicating that its MIC could be higher than the maximum tested value of 1000 µg/mL. Therefore, TF3 show limited or no bacteriostatic or bactericidal potential as a single agent within the tested concentration range. This result aligns with Kong et al. (2021), who observed that TF3 did not inhibit bacterial growth of *S. mutans* at the tested concentration up to 2500 µg/mL. Similarly for farnesol, according to Haj-Yahya et al. (2024) and Lobo et al. (2021), higher MIC values were reported at 50 µg/mL and 62.5 µg/mL against *S. mutans*, respectively. Nonetheless, Wang et al. (2019) reported that the MIC for TF3 against *S. mutans* was 62.5 µg/mL, with an MBC of 125 µg/mL. This discrepancy could be attributed to differences in experimental conditions, such as inoculum size, strain, growth phase, and the method of MIC determination, which can influence the concentration required for microbial inhibition.

Table 3. Result of MIC, MBC and FIC assays

Compounds	*S. mutans*		
	MIC (µg/mL)	**MBC (µg/mL)**	**FIC value**
TF3	> 1000	> 1000	ND
F	31.25	31.25	2
TF3-F	62.5	125	ND
Amoxicillin	<15.6	<15.6	NA

ND: Not determined; NA: Not applicable

Upon combination, TF3-F exhibited an MIC of 62.5 µg/mL and an MBC of 125 µg/mL, which are higher than those observed for F alone. These findings demonstrate that the combination of TF3 and F does not enhance the antibacterial activity of F alone. In fact, the MIC and MBC values for the TF3-F combination were higher than those of F used individually, indicating a reduction in potency when the compounds were combined. The interaction between TF3 and F against *S. mutans* was interpreted through the calculation of the Fractional Inhibitory Concentration Index (FICI). The FIC of F was calculated as 2.0. A previous study (Haj-Yahya et al., 2024) observed that farnesol enhanced the antimicrobial activity of AA against both *S. mutans* and *S. sobrinus*, with an FIC of 0.75, indicating an additive effect. Nonetheless, in the present study, since TF3 exhibited no measurable antibacterial activity, it is not possible to accurately determine its FIC. FICI interpretation requires clearly defined MIC values for both agents when used

individually, and the absence of the MIC value for TF3 renders any such calculation invalid. Therefore, the interaction between TF3 and F could not be classified as synergistic, additive, antagonistic or indifferent. Overall, these findings indicate that while farnesol alone is highly effective, the combination with TF3 does not reduce MIC or MBC values. This implies that the TF3-F combination may act through alternative mechanisms such as membrane disruption, modulation of quorum sensing signalling or biofilm inhibition, which were explored in the subsequent assays.

4.3 TIME KILLING KINETIC ANALYSIS

Time-killing assays provide dynamic insight into antimicrobial action by evaluating bacterial viability over time quantitatively. In this study, we employed 1× and 2× MIC concentrations of F and the TF3-F combination to determine their temporal bactericidal effects against *S. mutans*. Appendix I presents the time-kill kinetics of *S. mutans* treated with F and TF3-F combination over a six-hour incubation period. At 0 hours, all groups, including untreated and those treated with either F or TF3-F at 1× or 2× MIC, had the same bacterial count, with a $\log_{10}$ CFU/mL of 7.00. This confirms a consistent starting inoculum across all experimental conditions. Over time, rapid bacterial proliferation was observed in the untreated group, as it showed continuous bacterial growth. The CFU count increased to 7.35 $\log_{10}$ at 2 hours, reaching a peak of 12.71 $\log_{10}$ CFU/mL at 4 hours and slightly decreasing to 12.10 at 6 hours, indicating active and sustained proliferation of *S. mutans* in the absence of antimicrobial intervention. The slight reduction in bacterial growth may indicate that it had reached a saturation point or the end of the logarithmic growth phase.

In contrast, the TF3-F combination exhibited partial inhibitory effects. At 1× MIC, bacterial counts were moderately declined to 6.16 $\log_{10}$ at 2 hours, then decreased to 5.60 at 4 hours, and rose to 6.49 $\log_{10}$ at 6 hours. This pattern shows an initial inhibitory effect that was not sustained, indicative of regrowth and a lack of durable bactericidal activity at this concentration. At 2× MIC TF3-F, a stronger effect was observed, with the bacterial count decreased progressively to 5.11 $\log_{10}$ at 2 hours and 4.94 at 4 hours, remaining relatively stable at 5.02 by 6 hours. These findings indicate increased bacterial suppression at higher concentrations, but a lack of further reduction beyond 4 hours suggests that the TF3-F combination did not exert a fully bactericidal effect during the observed period.

The 1× MIC and 2× MIC F groups showed better killing activity against *S. mutans*. Both concentrations showed a consistent decrease in bacterial counts over time. At 1×MIC, the bacterial count dropped to 6.28 $\log_{10}$ at 2 hours, 5.87 at 4 hours, and 5.04 at 6 hours. Similarly, treatment with 2× MIC F reduced bacterial load to 5.69 $\log_{10}$ at 2 hours, 5.64 at 4 hours, and 4.60 at 6 hours. While the growth reduction was slightly less compared to TF3-F at 2 and 4 hours of treatment, the trend remained downward throughout the 6 hours, indicating continued bactericidal action without evidence of regrowth. This indicates that F was more effective than TF3-F in reducing the number of viable *S. mutans*, thereby supporting the qualitative results obtained from the MIC assay. Statistical analysis of the results revealed that all treatment groups were significantly different from the untreated control group ($p < 0.05$). Figure 8 displays the time-killing curve with Log_{10} CFU/mL on the Y-axis and incubation time on the X-axis.

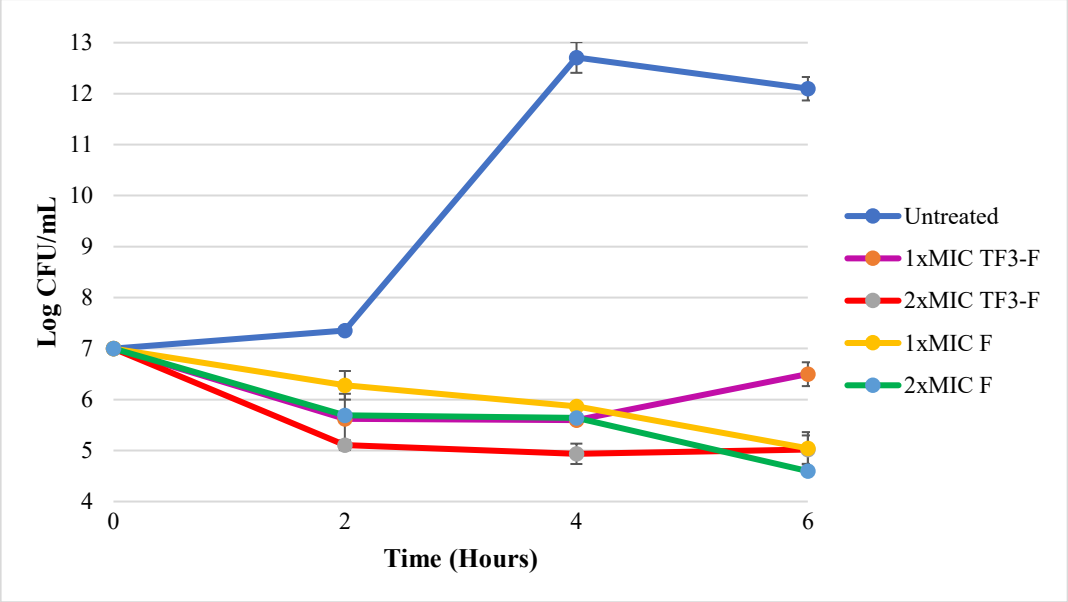

Figure 8. Time-killing curve of untreated and treated *S. mutans* over 6 hours

4.4 CELL MEMBRANE INTEGRITY ANALYSIS

The integrity of the bacterial cell membrane is a critical determinant of *S. mutans*' survival and pathogenicity. The membrane permeability assay, focused on measuring protein and nucleic acid leakage, is an essential test for evaluating the effects of antimicrobial agents on bacterial cell integrity. The assay measures the extent of cellular leakage of nucleic acids at OD_{260} and proteins at OD_{280}, providing insights into the disruption of membrane integrity. These parameters are well-established proxies for membrane disruption, as leakage of such macromolecules reflects loss of membrane selectivity and physical damage (Moo et al., 2021).

The membrane leakage assay, as shown in Appendix II, quantifies the extent of cellular leakage by measuring the release of nucleic acids at OD_{260} and proteins at OD_{280}

from *S. mutans* following treatments. One-way ANOVA was used to analyse the data, followed by Fisher's Least Significant Difference (LSD) Post-hoc test for multiple comparisons. In the untreated control group, the baseline leakage was recorded as 2.462 at OD_{260} and 1.553 at OD_{280}. These values serve as references for membrane integrity under normal, unchallenged conditions. *S. mutans* treated with F at both ¼× MIC and ½× MIC produced insignificant ($p > 0.05$) leakage of nucleic acid with OD_{260} values of 2.437 and 2.468, respectively, as compared to the untreated. Similarly, protein leakage values remained comparable to the control, with OD_{280} values of 1.247 for ¼× MIC of F and 1.546 for ½× MIC of F. These results suggest that at sublethal concentrations, F alone causes limited membrane disruption and induces negligible cellular content leakage.

In contrast, the TF3-F combination produced a markedly elevated leakage profile, particularly at ½ MIC. The OD_{260} value for ½ MIC was 3.037, indicating significant ($p < 0.05$) nucleic acid leakage as compared to the untreated, as shown in Figure 9. Meanwhile, protein leakage reached its highest level at an OD_{280} of 2.815, showing a significant increase ($p < 0.05$) to nearly twice the value observed in the untreated. Notably, even at ¼ MIC, the TF3-F treatment resulted in an increase of both nucleic acid and protein, with OD values of 2.790 and 2.402, respectively. These results suggest a substantial compromise of bacterial membrane integrity at sublethal concentrations of TF3-F.

Overall, the findings demonstrate that the TF3-F combination may induce more extensive membrane damage compared to F alone. The disruption is evident at both the nucleic acid and protein levels and is dose-dependent. Though TF3 alone was inactive, as evident in the MIC assay, it potentiates membrane-targeting activity when used in

combination with F. TF3-F combination induces pronounced membrane leakage, surpassing the effects of farnesol individually. This synergistic disruption of membrane integrity represents a key mechanistic advantage of the TF3-F formulation in weakening *S. mutans* pathogenicity.

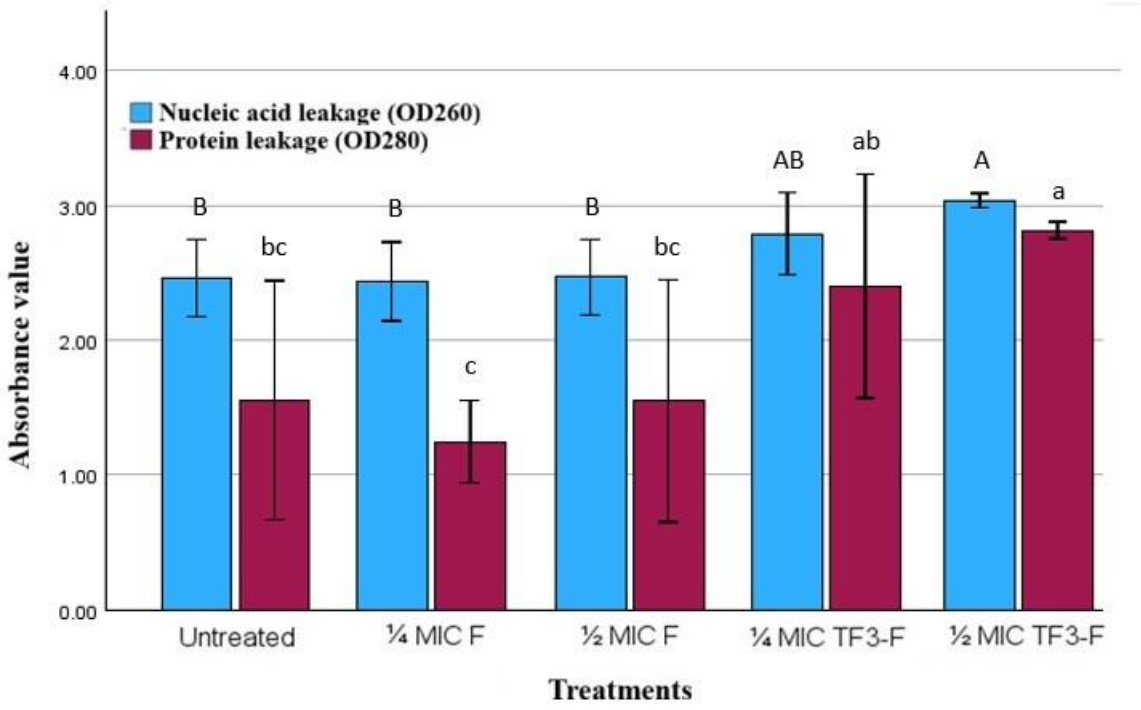

Figure 9. Leakage of nucleic acid and protein from treated and untreated *S. mutans*. Data represent the mean of triplicate readings and are expressed as Mean±SE. The mean was considered significantly different by different alphabets (a, b, c: Protein; A, B: Nucleic acid) at $p<0.05$.

4.5 CRYSTAL VIOLET UPTAKE

Table 4 presents the OD_{590} readings, which reflect the residual amount of CV in the supernatant, and the corresponding percentage of CV uptake by *S. mutans*. One-way ANOVA was used to analyse the data, followed by Tukey's Honest Significant

Difference (HSD) Post-hoc test for multiple comparisons. A higher OD_{590} denotes lower CV uptake, implying that the cell membrane remains mainly intact and impermeable. Conversely, a lower OD_{590} suggests increased membrane permeability, as more CV penetrates the compromised cells and is detectable less in the supernatant (Syal, K. 2017; Shui et al., 2021).

Table 4. Optical density and percentage of CV Uptake by *S. mutans*

Treatment	**OD_{590}**	**CV uptake (%)**
Untreated	0.154 ± 0.21	0%
¼ MIC F	0.095 ± 0.01	38.31 %
½ MIC F	0.068 ± 0.10	55.84 %
¼ MIC TF3-F	0.048 ± 0.01	68.83 %
½ MIC TF3-F	0.028 ± 0.15	81.82 %

The untreated control exhibited the highest OD_{590} value of 0.154 ± 0.21, serving as the baseline for an intact membrane integrity. *S. mutans* treated with ¼ MIC of F showed a reduction in OD_{590} to 0.095 ± 0.01, corresponding to a 38.31% increase in CV uptake, indicative of limited membrane disruption at this sublethal concentration. When the concentration was increased to ½ MIC F, the OD_{590} further decreased to 0.068 ± 0.10, which corresponds to a 55.84% of CV uptake, indicating a moderate membrane disruption in a dose-dependent manner (Jeon et al., 2011).

Notably, the TF3-F combination treatments showed more pronounced effects even at lower concentrations, as presented in Table 4. Treatment with ¼ MIC TF3-F resulted in an OD_{590} of 0.048 ± 0.01, corresponding to a 68.83% of CV uptake. This finding surpassed the effect of ½ MIC F alone, suggesting that TF3, although not bactericidal on its own, significantly enhances the membrane-disruptive potential of F. This trend was more prominent at ½ MIC TF3-F, where the OD_{590} dropped to 0.028 ± 0.15, corresponding to an 81.82% of CV uptake, which was the highest percentage of CV uptake. All treatments were statistically significant ($p<0.05$) difference from untreated, as shown in Figure 10.

This finding further highlights the potentiating role of TF3 on the permeabilising effect when used in combination, as observed in the membrane leakage assay. TF3 may facilitate the membrane-targeting actions of F, potentially weakening *S. mutans* without necessitating complete cell lysis. The lipophilic nature of farnesol and the amphiphilic nature of TF3 enable both molecules to interact favourably with the lipid components of *S. mutans* membranes. This interaction compromises membrane integrity and thus increases permeability. This approach may attenuate the bacterial virulence while minimising selective pressure for resistance (Inoue et al., 2016; Lin et al., 2024; Wang et al., 2019).

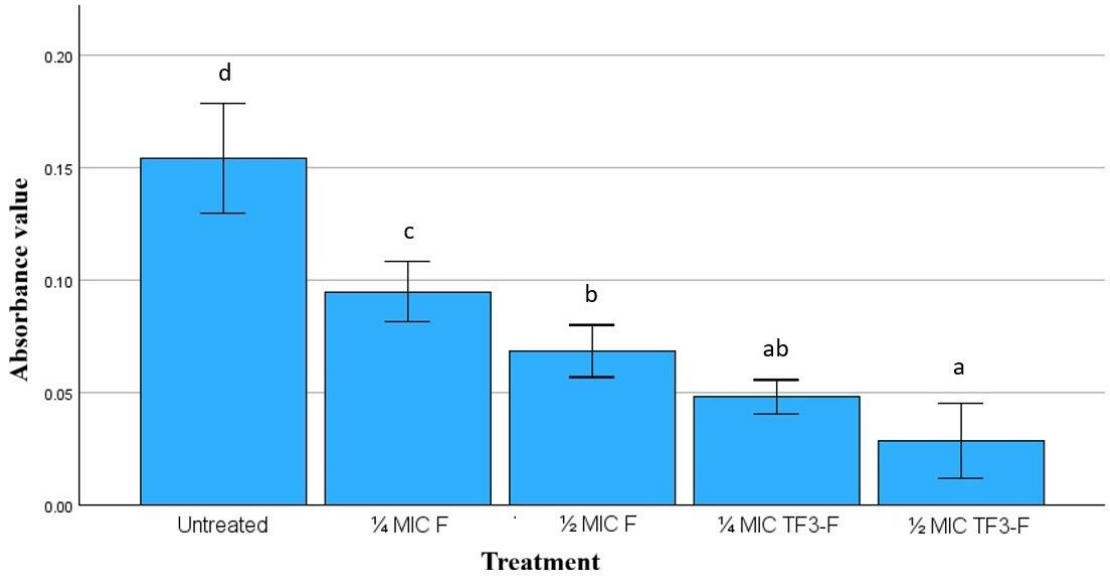

Figure 10. Optical density of the residual crystal violet in supernatant from treated and untreated *S. mutans*. Data represent the mean of triplicate readings and are expressed as Mean±SE. The mean was considered significantly different by different alphabets (a, b, c) at $p<0.05$.

4.6 ANTIBIOFILM INHIBITION EFFECTS

In this study, the biofilm inhibitory effects of farnesol and in combination with TF3 were tested at the concentration of ¼ MIC and ½ MIC. Table 5 presents both the OD_{570} values, which quantify the remaining biofilm mass following treatment, and the calculated percentage inhibition of biofilm relative to the untreated control. The untreated group recorded an OD_{570} of 0.471, establishing the baseline of biofilm formation without any treatment. One-way ANOVA was used to analyse the data, followed by Tukey HSD Post-hoc test for multiple comparisons.

Table 5. Result of anti-biofilm assay against *S. mutans*

Treatment	OD_{570}	Percentage of biofilm inhibition
Untreated	0.471 ± 0.98	0%
¼ MIC F	0.465 ± 0.24	1.27%
½ MIC F	0.341 ± 0.33	27.59%
¼ MIC TF3-F	0.335 ± 0.41	28.89%
½ MIC TF3-F	0.279 ± 0.21	40.77%

Treatment with ¼ MIC F resulted in an OD_{570} of 0.465, corresponding to only 1.27% inhibition. This negligible reduction indicates that at ¼ MIC, F alone exerts minimal impact on biofilm formation and is a statistically insignificant difference ($p>0.05$) from untreated, as shown in Figure 11. However, when the concentration was increased to ½ MIC F, a significant decrease ($p<0.05$) in OD_{570} to 0.341 was observed, corresponding to 27.59% inhibition. This indicates a dose-dependent effect, where higher concentrations of F lead to more pronounced biofilm inhibition. This increase in inhibition is consistent with a study done by Kashi et al. (2025), which found that higher concentrations of farnesol significantly impaired the formation of *S. mutans* biofilms.

Notably, the TF3-F combination demonstrated enhanced anti-biofilm effects even at lower doses and was statistically different ($p<0.05$) from the untreated. At ¼× MIC TF3-F, the OD_{570} value dropped to 0.335, with a biofilm inhibition of 28.89%. This

finding surpasses the anti-biofilm effect of ½× MIC F alone, suggesting a synergistic interaction between TF3 and F. At ½ MIC TF3-F, the OD_{570} further decreased to 0.279, which resulted in the highest biofilm inhibition, 40.77%, as presented in Figure 11. The observed effect may be attributed to the TF3, which may facilitate the penetration of farnesol by destabilising the biofilm matrix and inhibiting the biofilm formation (Wang et al., 2019; Fernandes et al., 2016)

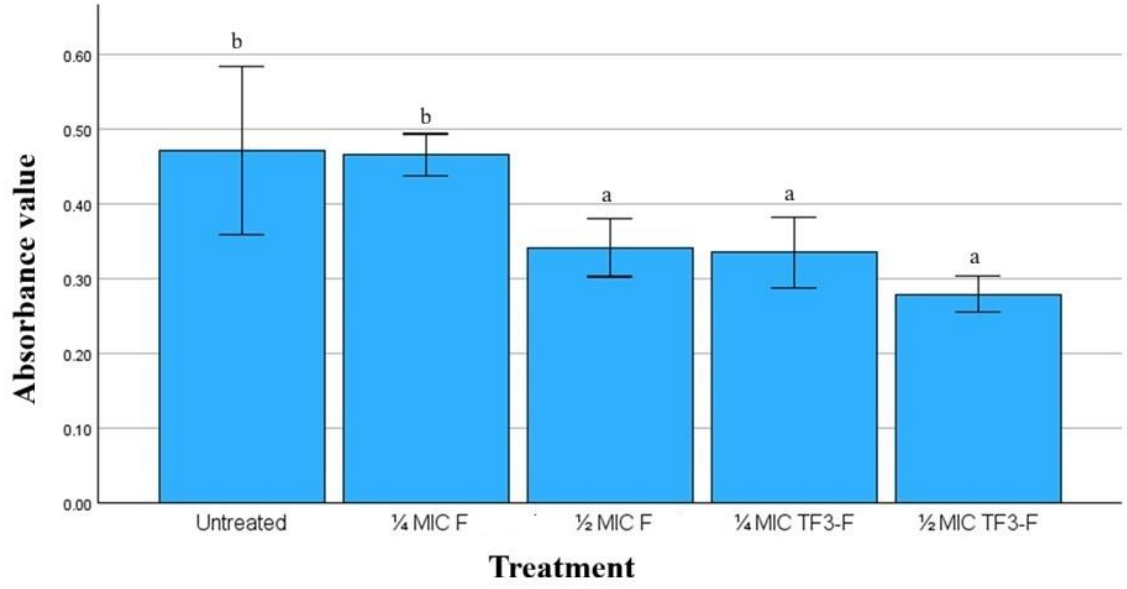

Figure 11. Absorbance reading of biofilm mass from treated and untreated *S. mutans*. Data represent the mean of triplicate readings and are expressed as Mean±SE. The mean was considered significantly different by different alphabets (a, b, c) at $p<0.05$.

4.7 MOLECULAR DOCKING ANALYSIS OF TF3 AND FARNESOL

In this study, molecular docking simulations were conducted to evaluate the binding interactions of TF3 and F with three quorum sensing (QS)-associated proteins of *S.*

mutans, namely S-ribosylhomocysteinase, response regulator ComE, and ATP-binding cassette transporter ComA. These targets represent important regulatory and enzymatic components involved in quorum sensing and biofilm formation in *S. mutans* (Li et al., 2012; Ishii et al., 2017; Kaur et al., 2015). To validate the docking protocol, positive controls were included for each target. Baicalein, an inhibitor of LuxS (Mao et al., 2023), was used for S-ribosylhomocysteinase, and ATP, the natural substrate of ComA (Ishii et al., 2013), was used for the ATP-binding cassette transporter ComA. 2-Aminoimidazole (2-AI) was selected as a reference ligand for docking against ComE based on prior evidence that 2-AI compounds bind to the response regulator *VicR* in *S. mutans* and inhibit biofilm formation (Liu et al., 2023). Although direct binding to ComE has not been reported, the structural similarity among response regulators provides a rationale for its use as a tentative positive control. Table 6 shows the molecular docking results of TF3 and F against the selected QS-associated proteins of *S. mutans*.

Figure 12 illustrates the 2D interaction between TF3 and 4XCH. TF3 exhibited the lowest binding energy among all ligands tested (−10.08 kcal/mol) and formed the most hydrogen bonds (11) with protein residues. The interactions involved multiple critical residues, including Cys82, which is the predicted active residue. In contrast, F had a higher binding energy of −5.39 kcal/mol and formed only three hydrogen bonds, involving Cys82 (2.22 Å and 2.42 Å) and Glu60 (1.98 Å), as shown in Figure 13. The limited interactions with most of the catalytic residues suggest that F binds less stably to 4XCH than TF3. Shi et al. (2025), and Asano et al. (2024) reported that compounds exhibiting weaker binding affinities, particularly those interacting with non-conserved residues, are less likely to effectively inhibit the function of target proteins. However,

other studies demonstrated that compounds binding to allosteric sites, regions which are distinct from the active site, can significantly modulate protein activity through allosteric regulation (Guo & Zhou, 2016; Guarnera & Berezovsky, 2016).

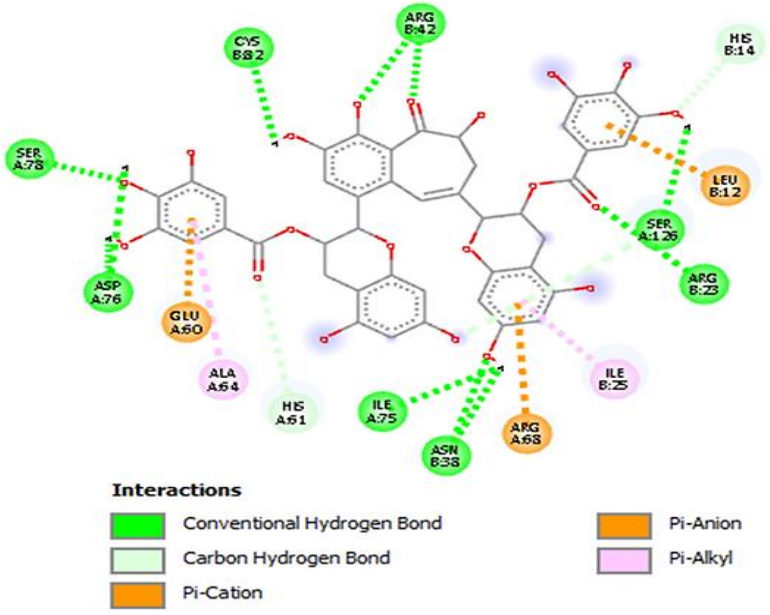

Figure 12. 2D diagram of TF3 interaction with S-ribosylhomocysteinase

Table 6. Molecular docking result of TF3 and F against quorum sensing-associated proteins of *S. mutans*

Ligands	**Binding Energy (kcal/mol)**	**Number of H-bonds**	**H-bonded residues with distance (Å)**
PBD 4XCH (S-ribosylhomocysteinase)			
Active site: His57, His61, Cys82, Cys127			
Baicalein	−7.57±0.29	4	**His57 (2.98)**, Cys77(2.60 & 2.67), His87 (2.88)
TF3	−10.08±0.45	11	Ser78(2.15), Asp76(2.41), Asp76(2.11) **Cys82(2.91)**, Arg42(2.45), Arg 42(2.40), Ser 126 (2.43), Arg23(2.74), Ile75(2.38), Asn38(2.86), Asn38(2.54)
F	−5.39±0.21	3	**Cys82(2.22)**, **Cys82(2.42)**, Glu60(1.98)
PBD 4MLD (ComE)			
Active Site: Glu58, Phe86, Phe93, Tyr98, Phe107			
2-AI	−3.97±0.06	2	Ser91(2.35), Glu92(2.19)
TF3	−4.28±0.48	2	**Phe107**(2.75 & 2.12)
F	−4.46±0.26	1	Ile84(3.05)
PBD 3VX4 (ComA)			
Active site: Tyr537, Lys567, Ser666, Asp689, Ala690, His720			
ATP	−8.40±0.35	8	Gly668(2.20), Thr569(1.59), Thr568(1.57), Thr568(2.76), **Lys567(2.03)**, Gln669(2.01), Ser565(2.22), Asp542(2.65)
TF3	−9.14±0.56	5	Thr543(2.14), Glu658(2.27**)**, **Tyr537(2.82)**, Gly538(1.91), Gln669(1.87)
F	−5.57±0.14	3	Ala611(2.77), Ala611(2.87), Gln610(2.19)

2-AI = 2-Aminoimidazoles

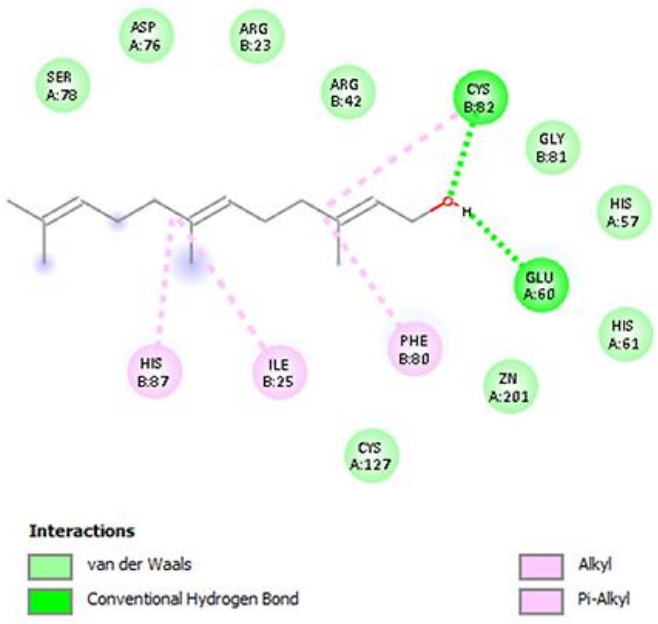

Figure 13. 2D diagram of F interaction with S-ribosylhomocysteinase

Figure 14 illustrates the 2D interaction between TF3 and ComE. TF3 exhibited a binding energy of −4.28 kcal/mol, forming two hydrogen bonds with ComE residues. These interactions primarily involved Phe107 at distances of 2.75 Å and 2.12 Å. Meanwhile, F had a slightly weaker binding energy of −4.46 kcal/mol and formed a single hydrogen bond with Ile84 (3.05 Å). The interaction with a non-active residue (Ile84) and an extended bond length (>3.0 Å) may imply that the interaction is weak and likely contributes minimally to binding stability. This weak interaction suggests that F is unlikely to directly affect ComE activity or function as a quorum sensing inhibitor. Figure 15 shows the limited interaction of F to the functional site of ComE, with an H-bond stabilising the ligand.

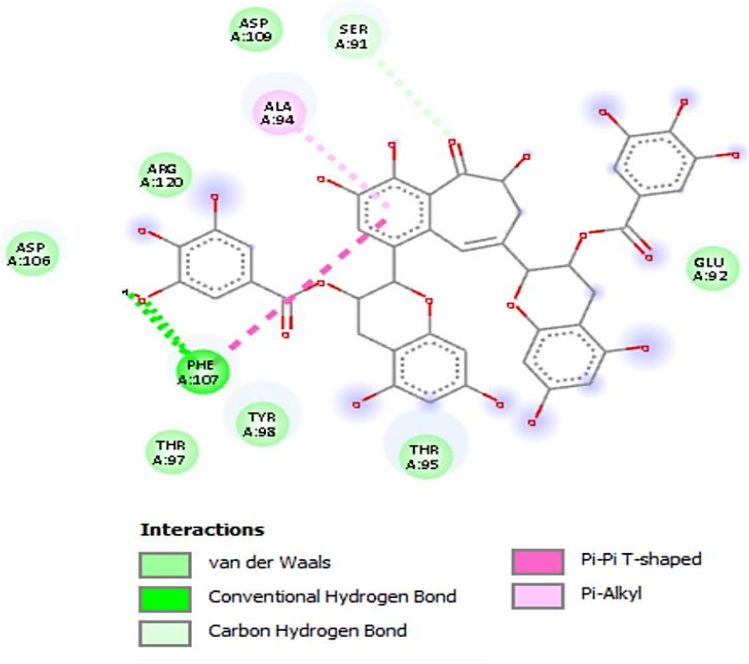

Figure 14. 2D diagram of TF3 interaction with ComE

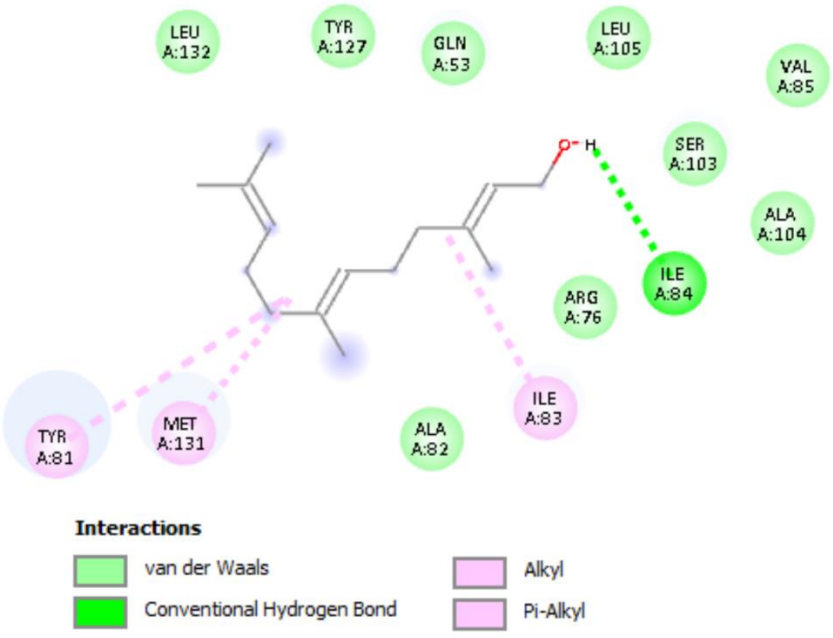

Figure 15. 2D diagram of F interaction with ComE

ComA serves as a key mediator in the initiation of quorum sensing, primarily responsible for exporting the competence-stimulating peptide (CSP) precursor, encoded by ComC, from the cytoplasm (Yu et al., 2023). TF3 demonstrated a high affinity for ComA, exhibiting a binding energy of −9.14 kcal/mol and forming five hydrogen bonds with the residues, including Tyr537 (2.82 Å), which is one of the protein's active residues. Figure 16 illustrates TF3's formation of multiple polar and hydrophobic interactions within the ComA structure, highlighting its potential to disrupt regulatory functions related to quorum sensing and competence development in *S. mutans*. In comparison, F exhibited a weaker binding energy of −5.57 kcal/mol. As shown in Figure 17, F formed three conventional hydrogen bonds with Gln610 and Ala611, neither of which is among the key active-site residues (Tyr537, Lys567, Ser666, Asp689, Ala690, and His720) involved in the interaction.

Overall, the limited number of short-range hydrogen bonds and the lack of interaction with active residues suggest that F binds weakly and nonspecifically to the target proteins. Despite forming a few hydrogen and hydrophobic interactions, it does not establish strong or targeted interactions within the functional domain of the proteins. In contrast, TF3 demonstrates a greater ability to specifically interact with QS-associated proteins, particularly ComA and S-ribosylhomocysteinase, suggesting a higher potential to effectively disrupt bacterial communication and biofilm formation (Guzmán-Flores et al., 2024).

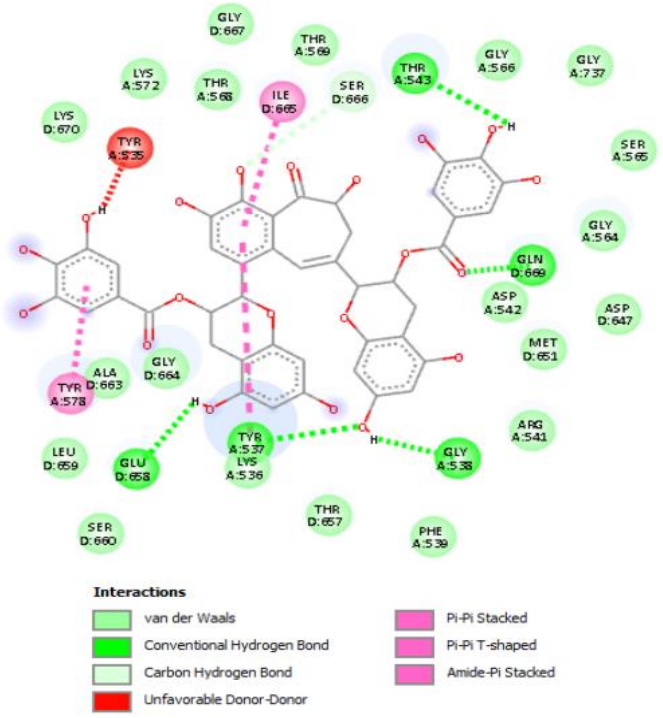

Figure 16. 2D diagram of TF3 interaction with ComA

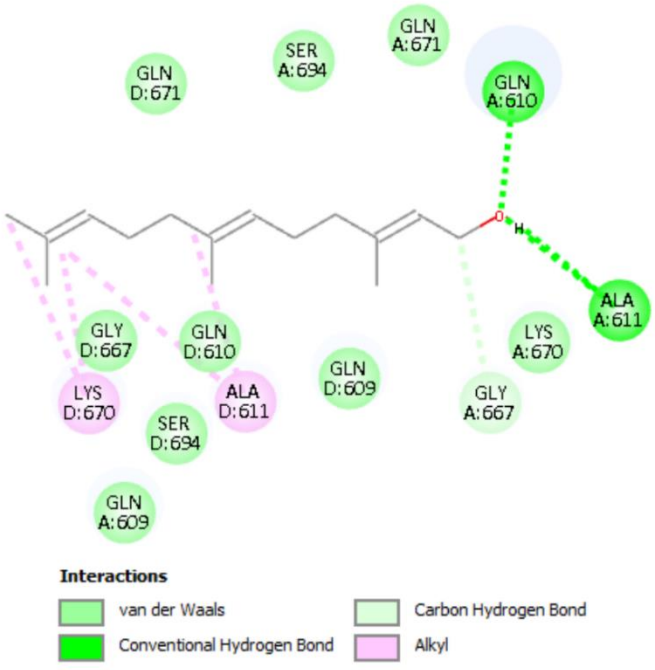

Figure 17. 2D diagram of F interaction with ComA

4.8 FIELD EMISSION SCANNING ELECTRON MICROSCOPY (FESEM) ANALYSIS

Field emission scanning electron microscopy (FESEM) is a high-resolution imaging technique widely used to examine morphological changes in microorganisms under various treatment conditions (Robles-Gómez et al., 2025). In this study, FESEM images of untreated and treated *S. mutans* were observed at magnifications of 10,000×, 20,000×, and 30,000× under an accelerating voltage of 5.0 kV. Figure 18 shows the SEM images of untreated *S. mutans* at a magnification of 20,000×, exhibiting coccoid-shaped cells that were densely aggregated in clusters. The cell surfaces were smooth, uniform, and intact, with no signs of rupture, collapse, or deformation. These morphological characteristics are in line with previous observations reported by Yue et al. (2018), who similarly described untreated *S. mutans* as exhibiting well-defined, spherical morphology with compact clustering and smooth surface architecture.

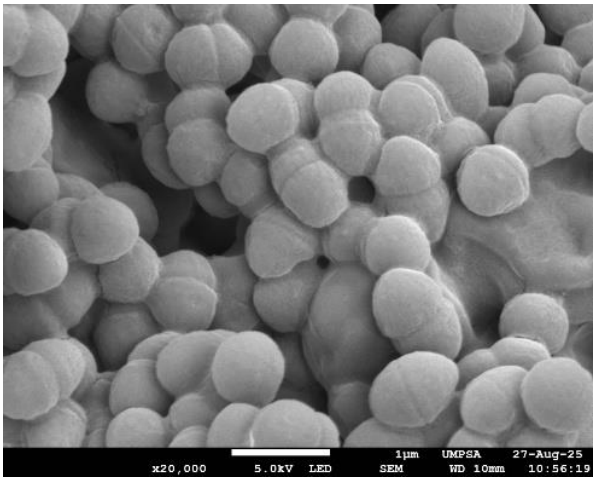

Figure 18. FESEM image of untreated *S. mutans* observed at magnification of 20,000×

In contrast, *S. mutans* treated with ¼× MIC and ½× MIC of F exhibited progressive and dose-dependent alterations in cellular morphology. At ¼× MIC of F, the bacterial population appeared heterogeneous, with many cells displaying irregular outlines, variable sizes, and reduced compactness within clusters. The surface architecture remained mostly smooth but showed areas of roughening, wrinkling, and uneven textures, with occasional elongated cells observed. At ½× MIC of F, these morphological disruptions became more pronounced, as clusters appeared noticeably less compact with visible intercellular gaps. The cell surfaces appeared rough, corrugated, and irregular, with the presence of aggregated surface deposits, indicating potential compromise of the cell integrity. The cell surfaces appeared markedly roughened, corrugated, and uneven, with localised depressions or collapses as shown in Figure 19.

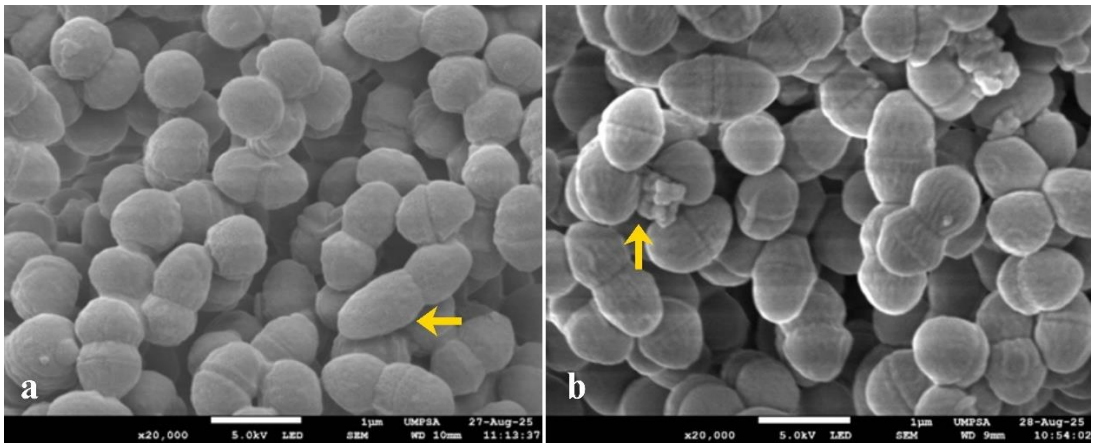

Figure 19. FESEM image of *S. mutans* treated with ¼× MIC (a) and ½× MIC (b) of F at a magnification of 20,000×. Morphological changes were indicated by arrows at the affected cells.

Following these observations, the morphology of *S. mutans* treated with the TF3–F combination at ¼× and ½× MIC revealed more extensive and compounded cellular alterations compared to farnesol alone. As illustrated in Figure 20, the cell surfaces appeared markedly roughened, corrugated, with vesicle-like protrusions, surface blebs, and localised depressions or collapses at ¼×MIC of TF3-F. Meanwhile, at ½× MIC of TF3-F, the extent of deformation was visibly greater, characterised by pronounced membrane collapse, presence of aggregated surface deposits, blebs and tearing, indicating severe loss of cellular integrity.

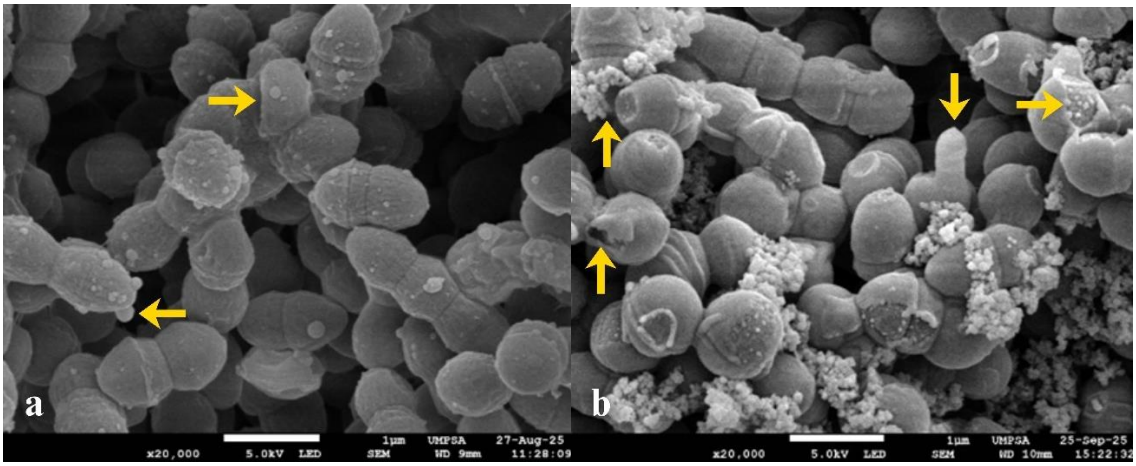

Figure 20. FESEM image of *S. mutans* treated with ¼× MIC (a) and ½× MIC (b) of TF3-F at a magnification of 20,000×. Morphological changes were indicated by arrows at the affected cells.

The severe morphological changes correspond to advanced stages of membrane destabilisation and stress response, indicating that the combination treatment of TF3-F compromises the physical and functional stability of the cell. Comparable findings have been reported by Zheng et al. (2018), who demonstrated that exposure to tea polyphenol-

based materials induced roughened surfaces, depressions, and partial collapse of *S. mutans* cells, while Li et al. (2013) associated such structural deformation with peptidoglycan disruption and subsequent cytoplasmic leakage.

In this study, the presence of collapsed, vesiculated, and shrunken cells under the TF3-F treatment strongly supports the occurrence of intracellular leakage and weakening of membrane integrity. The progressive nature of this damage suggests that the combination exerts a synergistic destabilising effect on the bacterial membrane, facilitating the release of cytoplasmic constituents. These findings are in agreement with the increased absorbance at 260/280 nm recorded in the leakage assay, signifying nucleic acid and protein efflux. In sum, the FESEM results provide visual confirmation that the TF3-F combination severely disrupts *S. mutans* morphology and membrane integrity, extending beyond the effects of farnesol alone, even at a sublethal concentration, as illustrated in Figure 21.

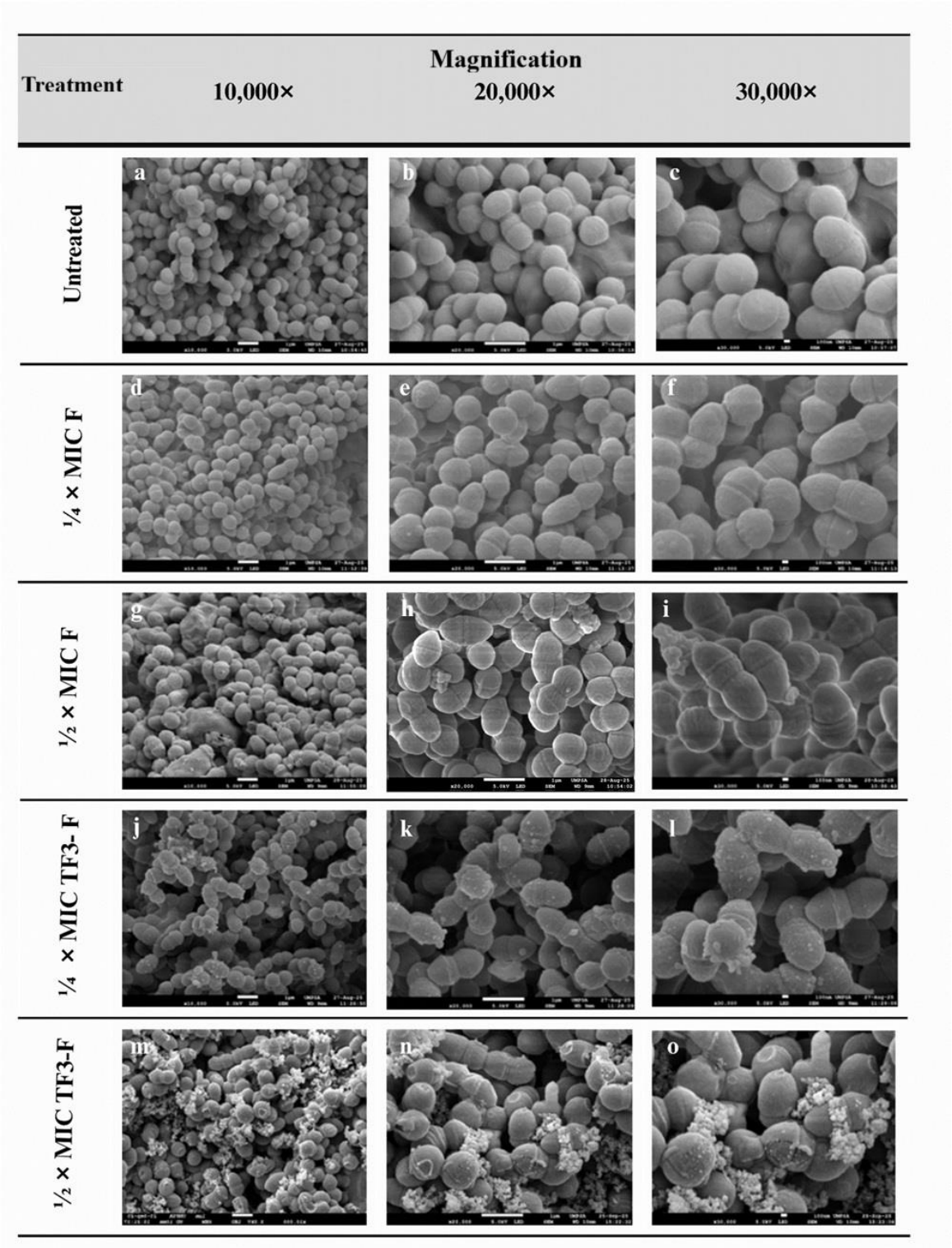

Figure 21. FESEM images of untreated and treated *S. mutans* at sub-lethal concentrations of farnesol (F) and TF3-F combination at magnifications of 10,000×, 20,000×, and 30,000×.

CHAPTER 5

CONCLUSION AND FUTURE DIRECTION

This study elucidated the antibacterial effects of farnesol (F), TF3 and their combination at sublethal concentrations against *S. mutans*, a primary pathogen implicated in ECC. The findings demonstrated that while TF3, a polyphenolic compound, exhibited no detectable inhibitory effect at concentrations up to 1000 µg/mL, its combination with farnesol enhanced antibacterial efficacy through intricate mechanisms targeting biofilm formation, membrane integrity, and quorum sensing.

The MIC and MBC values of the TF3-F combination were higher than those of farnesol alone, indicating reduced antibacterial potency in terms of growth inhibition. However, the TF3-F combination demonstrated notable effects on *S. mutans* virulence-related properties, suggesting potential multi-target interactions rather than synergistic activity. Time-kill assay of the TF3-F combination indicated a concentration-dependent inhibitory trend, with partial growth suppression rather than sustained bactericidal activity. Meanwhile, the membrane leakage assays confirmed progressive disruption of cell membrane integrity. Increased absorbance at 260 nm and 280 nm reflected the release of intracellular nucleic acids and proteins, corroborating the membrane-compromising effects of the TF3-F combination in FESEM analysis.

Molecular docking analyses provided further mechanistic insight, revealing that TF3 demonstrated strong binding affinities and stable hydrogen bond interactions with quorum sensing-associated proteins, particularly ComA, LuxS, and glycosyltransferase homologs. Since quorum sensing regulates biofilm formation and stress adaptation in *S.*

mutans, the predicted interactions of TF3 with quorum sensing associated proteins suggest possible interference with these signalling pathways. This interference may underlie the observed *in vitro* effects of TF3-F, including reduced biofilm biomass and compromised membrane integrity. Specifically, protein and nucleic acid leakage assay, crystal violet uptake assay and anti-biofilm assay demonstrated that the TF3-F combination exhibits higher antimicrobial activity compared to farnesol alone.

The significance of this study lies in its demonstration that natural compounds at sublethal concentrations may modulate the pathogenicity of *S. mutans* without imposing strong selective pressure for resistance. This "disarming without killing" approach aligns with the growing paradigm of anti-virulence therapy, which seeks to modulate pathogenic behaviour instead of eradicating microbial populations. By disrupting quorum sensing and destabilising the bacterial membrane, the TF3-F combination offers a promising strategy for attenuating *S. mutans* virulence while preserving the ecological balance of the oral microbiome and reducing the likelihood of resistance development. Such findings highlight its potential relevance in the prevention of ECC through targeted modulation of bacterial pathogenicity.

Furthermore, while this study has provided valuable insights into the antibacterial and membrane-disruptive effects of the TF3-F combination against *S. mutans*, further research is required to confirm its efficacy beyond the *in vitro* setting. Future investigations should aim to elucidate the precise molecular pathways associated with the observed membrane damage and its downstream influence on quorum sensing, gene regulation, and biofilm dynamics. Detailed transcriptomic and proteomic analyses are recommended to identify the global gene networks and signalling cascades affected by

TF3-F exposure. Particular attention should be given to the modulation of quorum sensing genes (*comCDE*, *luxS*), glucosyltransferase genes (*gtfB*, *gtfC*), and acid-tolerance regulators (*atpD*, *vicRK*), as these pathways are pivotal to *S. mutans* virulence and ecological persistence.

To bridge the gap between laboratory findings and clinical relevance, *in vivo* studies using established caries-inducing models are essential to evaluate the biocompatibility, safety, and therapeutic potential of TF3-F within the complex oral microbiome. Such models would allow assessment of their capacity to suppress *S. mutans* colonisation and reduce lesion development under realistic oral conditions. Beyond mechanistic exploration, translational research should focus on incorporating TF3-F into practical oral care prototypes such as mouthwashes, toothpastes, mucoadhesive gels, or varnish formulations. These delivery systems would facilitate sustained retention and gradual release on tooth surfaces, thereby maximising preventive efficacy.

In parallel, the development of nanoparticle-based or polymer-encapsulated formulations could improve the stability and bioavailability of TF3-F, ensuring prolonged activity in the oral cavity. Exploring synergistic interactions with conventional anticaries agents, including fluoride or other bioactive compounds, may further enhance its preventive potential. Finally, longitudinal clinical trials are needed to validate the safety, stability, and long-term effectiveness of TF3-F in reducing *S. mutans* load and caries incidence. Collectively, these future directions are crucial for translating promising in vitro findings into clinically applicable, biocompatible strategies for sustainable ECC prevention and improved paediatric oral health outcomes.

REFERENCES

Adeghe, E. P. (2024). The multifaceted role of fluoride in preventing early childhood caries: A comprehensive review. *International Journal of Life Science Research Updates, 2*(1), 9–17.

Akram, M. E., Jahangir, U., Aziz, I., Shahzad, M. N., Jehangir, M., Kashif, M. B., & Rashid, A. (2025). Biofilm formation in dental caries and advancements in biofilm-targeted therapies: A decade of progress. *Journal of Health, Wellness, and Community Research,* e135–e135.

Alamoudi, R. A. (2025, May). Bibliometric analysis of cross-sectional studies on early childhood caries. In *Healthcare* (Vol. 13, No. 9, p. 1067). MDPI.

Alfhili, M. A., Hussein, H. A., Park, Y., Lee, M. H., & Akula, S. M. (2021). Triclosan induces apoptosis in Burkitt lymphoma-derived BJAB cells through caspase and JNK/MAPK pathways. *Apoptosis, 26*(1), 96–110.

Almoudi, M. M., Hussein, A. S., Abu-Hassan, M. I., Saripudin, B., & Mohamad, M. S. F. (2021). The association of early childhood caries with salivary antimicrobial peptide LL37 and *mutans streptococci*. *Journal of Clinical Pediatric Dentistry, 45*(5), 330–336.

Anderson, A. C., Al-Ahmad, A., Schlueter, N., Frese, C., Hellwig, E., & Binder, N. (2020). Influence of the long-term use of oral hygiene products containing stannous ions on the salivary microbiome–a randomized controlled trial. *Scientific reports*, *10*(1), 9546.

Anil, S., & Anand, P. S. (2017). Early childhood caries: Prevalence, risk factors, and prevention. *Frontiers in Pediatrics, 5*, 157.

Asano, W., Hantani, R., Uhara, T., Debaene, F., Nomura, A., Yamaguchi, K., Adachi, T., Otake, K., Harada, K., & Hantani, Y. (2024). Screening approaches for the identification of Nrf2–Keap1 protein–protein interaction inhibitors targeting hot spot residues. *SLAS Discovery, 29*(2), Article 100125.

Baker, J. L., Abranches, J., Faustoferri, R. C., Hubbard, C. J., Lemos, J. A., Courtney, M. A., & Quivey, R. G., Jr. (2015). Transcriptional profile of glucose-shocked and acid-adapted strains of *Streptococcus mutans*. *Molecular Oral Microbiology, 30*(6), 496–517.

Chen, J., & Zhang, W. (2025). Advances in antimicrobial, antibiofilm, and remineralization strategies against oral *Streptococcus mutans* found in natural and synthetic agents. *Journal of Biosciences and Medicines, 13*(4), 16–25.

Çoğulu, D., Aşık, A., Yılmaz Süslüer, S., Yücel Er, C., Topaloğlu, A., Uzel, A., & Gündüz, C. (2025). *In vitro* analysis of various mouthwashes: Cytotoxic, apoptotic, genotoxic, and antibacterial effects. *Clinical Oral Investigations, 29*(4), 1–10.

Choi, Y.-S., Kim, J.-Y., Nah, H.-R., Seo, B.-G., An, D.-H., You, J.-W., Lee, S.-E., & Nam, S.-H. (2017). Anti-caries effect of the *Glycyrrhiza uralensis* extract. *Biomedical Research (India), 28*(19), 8271–8275.

Costa, A. F., da Silva, J. T., Martins, J. A., Rocha, V. L., & Amaral, A. C. (2025). Chitosan nanoparticles encapsulating farnesol show potent antifungal activity against *Candida albicans* biofilms. *Brazilian Journal of Microbiology, 56*(2), 905–912.

Dang, M.-H., Jung, J.-E., Lee, D.-W., Song, K.-Y., & Jeon, J.-G. (2016). Recovery of acid production in *Streptococcus mutans* biofilms after short-term fluoride treatment. *Caries Research, 50*(4), 363–371.

Decker, E.-M., Klein, C., Schwindt, D., & Von Ohle, C. (2014). Metabolic activity of *Streptococcus mutans* biofilms and gene expression during exposure to xylitol and sucrose. *International Journal of Oral Science, 6*(4), 195–204.

Deus, F. P., & Ouanounou, A. (2022). Chlorhexidine in dentistry: Pharmacology, uses, and adverse effects. *International Dental Journal, 72*(3), 269–277.

Dharsini, S., Ramakrishnan, M., & Ganapathy, D. (2020). The effect of severe caries on the quality of life in young children: A cross-sectional study. *Drug Invention Today, 14*(3), 1–5.

Dinis, M., Agnello, M., Cen, L., Shokeen, B., He, X., Shi, W., Wong, D. T. W., Lux, R., & Tran, N. C. (2022). Oral microbiome: *Streptococcus mutans*/caries concordant-discordant children. *Frontiers in Microbiology, 13*, Article 782825.

Du, X., Zhang, J., & Zhang, L. (2025). A comprehensive review of theaflavins: Physiological activities, synthesis, and applications. *Food Science & Nutrition, 13*(1), e15458.

Dutta, S., & Mohapatra, A. (2022). Early childhood caries—Etiology, prevention and management: A review. *Archives of Dental Research, 12*(2), 81–88.

Fadhlina, A., Sheikh, H. I., & Lestari, W. (2023). Molecular docking studies of an isolated angucycline of *Stereospermum fimbriatum*, a novel anti-MRSA agent. *Malaysian Journal of Fundamental and Applied Sciences, 19*(4), 553–562.

Farah, H., Steinberg, D., & Sionov, R. V. (2024). Trans, trans-farnesol enhances the anti-bacterial and anti-biofilm effect of arachidonic acid on the cariogenic bacteria *Streptococcus mutans* and *Streptococcus sobrinus*. *International Journal of Molecular Sciences*, *25*(11), 11770.

Fernandes, R. A., Monteiro, D. R., Arias, L. S., Fernandes, G. L., Delbem, A. C. B., & Barbosa, D. B. (2016). Biofilm formation by *Candida albicans* and *Streptococcus mutans* in the presence of farnesol: A quantitative evaluation. *Biofouling, 32*(3), 329–338.

Gao, Z., Chen, X., Wang, C., Song, J., Xu, J., Liu, X & Suo, H. (2024). New strategies and mechanisms for targeting *Streptococcus mutans* biofilm formation to prevent dental caries: A review. *Microbiological Research, 278*, 127526.

Guarnera, E., & Berezovsky, I. N. (2016). Allosteric sites: Remote control in regulation of protein activity. *Current Opinion in Structural Biology, 37*, 1–8.

Guo, J., & Zhou, H.-X. (2016). Protein allostery and conformational dynamics. *Chemical Reviews, 116*(11), 6503–6515.

Guzmán-Flores, J. M., Pérez-Reyes, Á., Vázquez-Jiménez, S. I., Isiordia-Espinoza, M. A., & Martínez-Esquivias, F. (2024). A docking and network pharmacology study on the molecular mechanisms of curcumin in dental caries and *Streptococcus mutans*. *Dentistry Journal, 12*(6), 153.

Hacioglu, M., Yilmaz, F. N., Yetke, H. I., & Haciosmanoglu-Aldogan, E. (2024). Synergistic effects of quorum-sensing molecules and antimicrobials against *Candida albicans* and *Pseudomonas aeruginosa* biofilms: in vitro and in vivo studies. *Journal of Antimicrobial Chemotherapy*, 79(11), 2828-2836.

Haj-Yahya, F., Steinberg, D., & Sionov, R. V. (2024). Trans, trans-farnesol enhances the anti-bacterial and anti-biofilm effect of arachidonic acid on the cariogenic bacteria *Streptococcus mutans* and *Streptococcus sobrinus*. *International Journal of Molecular Sciences*, 25(21), 11770.

Halden, R. U., Lindeman, A. E., Aiello, A. E., Andrews, D., Arnold, W. A., Fair, P., ... & Blum, A. (2017). The Florence statement on triclosan and triclocarban. *Environmental health perspectives*, *125*(6), 064501.

Halder, S., Yadav, K. K., Sarkar, R., Mukherjee, S., Saha, P., Haldar, S., Karmakar, S. & Sen, T. (2015). Alteration of Zeta potential and membrane permeability in bacteria: a study with cationic agents. *SpringerPlus*, 4(1), 672.

Hossain, M. N., Shamrin, T., Jannat, T., Ahmed, B., Islam, S., & Rahman, M. A. (2025). Dental caries – Microbiological investigation in patients attending a dental clinic. *Molecular Mechanism Research*, 3(1), 8887.

Huo, Y., Mai, J., Ling, J., & Huo, L. (2011). Effects of *immA* and *immB* coding putative bacteriocin immunity proteins on the antimicrobial sensitivity in planktonic *Streptococcus mutans* and biofilm formation. *Zhonghua Kou Qiang Yi Xue Za Zhi = Chinese Journal of Stomatology, 46*(8), 478–483.

Hu, X., Ping, Z., Gan, M., Tao, Y., Wang, L., Shi, J., ... & Geng, D. (2017). Theaflavin-3, 3′-digallate represses osteoclastogenesis and prevents wear debris-induced osteolysis via suppression of ERK pathway. Acta Biomaterialia, 48, 479-488.

Huang, J., Fan, Y., Lei, Z., Yu, Z., Ni, D., & Chen, Y. (2023). The inhibitory effect and mechanism of theaflavins on fluoride transport and uptake in HIEC-6 cell model. *Food and Chemical Toxicology*, 178, 113939.

Inoue, Y., Togashi, N., & Hamashima, H. (2016). Farnesol-induced disruption of the *Staphylococcus aureus* cytoplasmic membrane. *Biological and Pharmaceutical Bulletin, 39*(5), 653–656.

Ishii, S., Yano, T., Okamoto, A., Murakawa, T., & Hayashi, H. (2013). Boundary of the nucleotide-binding domain of *Streptococcus* ComA based on functional and structural analysis. *Biochemistry*, 52(15), 2545-2555.

Ishii, S., Fukui, K., Yokoshima, S., Kumagai, K., Beniyama, Y., Kodama, T., Fukuyama, T., Okabe, T., Nagano, T., Kojima, H., & Yano, T. (2017). High-throughput screening of small molecule inhibitors of the *Streptococcus* quorum-sensing signal pathway. *Scientific Reports, 7*(1), Article 4029.

Jawdekar, A. M., Shirke, K. J., & Mitra, M. (2024). Sustainable Clinical Management of Dental Caries: A Global Snapshot of Prevalence, Prognosis and Management. *Journal of Pediatrics, Perinatology and Child Health*, *8*, 172-180.

Jeon, J.-G., Pandit, S., Xiao, J., Gregoire, S., Falsetta, M. L., Klein, M. I., & Koo, H. (2011). Influences of *trans-trans* farnesol, a membrane-targeting sesquiterpenoid, on *Streptococcus mutans* physiology and survival within mixed-species oral biofilms. *International Journal of Oral Science, 3*(2), 98–106.

Jiang, Q., Xu, M., Chen, H., Zhang, Y., Sun, Y., Tao, L., ... & Yang, D. (2025). V-ATPase contributes to the cariogenicity of Candida albicans-Streptococcus mutans biofilm. *npj Biofilms and Microbiomes*, *11*(1), 41.

Jurczak, A., Jamka-Kasprzyk, M., Bębenek, Z., Staszczyk, M., Jagielski, P., Kościelniak, D., Gregorczyk-Maga, I., Kołodziej, I., Kępisty, M., Kukurba-Setkowicz, M., Bryll, A., & Krzyściak, W. (2020). Differences in sweet taste perception and its association with the *Streptococcus mutans* cariogenic profile in preschool children with caries. *Nutrients, 12*(9), 2592.

Kamarehei, F., Mehdiabadi, M., & Naderi, F. (2022). Antibacterial effects of natural compounds on biofilm formation of *Streptococcus mutans*. *Clinical and Experimental Dental Research*, 8(6), 1426-1433.

Kashi, M., Varseh, M., Hariri, Y., Chegini, Z., & Shariati, A. (2025). Natural compounds: new therapeutic approach for inhibition of *Streptococcus mutans* and dental caries. *Frontiers in Pharmacology*, 16, 1548117.

Kaur, G., Rajesh, S., & Princy, S. A. (2015). Plausible drug targets in the *Streptococcus mutans* quorum-sensing pathways to combat dental biofilms and associated risks. *Indian Journal of Microbiology, 55*(4), 349–356.

Kimijima, M., Narisawa, N., Hori, E., Mandokoro, K., Ito, T., Ota, Y., Sashida, M., Kawai, Y., & Takenaga, F. (2024). Nattokinase, a subtilisin-like alkaline-serine protease, reduces mutacin activity by inactivating the competence-stimulating peptide in *Streptococcus mutans*. *Pathogens, 13*(4), Article 286.

Kong, J., Xia, K., Su, X., Zheng, X., Diao, C., Yang, X., Zuo, X., Xu, J., & Liang, X. (2021). Mechanistic insights into the inhibitory effect of theaflavins on virulence factors production in *Streptococcus mutans*. *AMB Express, 11*(1), Article 102.

Lemme, A., Sztajer, H., & Wagner-Döbler, I. (2010). Characterization of *mleR*, a positive regulator of malolactic fermentation and part of the acid tolerance response in *Streptococcus mutans*. *BMC Microbiology, 10*, Article 58.

Li, Q., Shen, J., Qin, T., Zhou, G., Li, Y., Chen, Z., & Li, M. (2021). A qualitative and comprehensive analysis of caries susceptibility for dental fluorosis patients. Antibiotics, 10(9), 1047.

Li, H., Zhao, H., Zhu, L., Hong, L., Zhang, H., Lin, F., Xu, C., Li, S., & Zhang, Z. (2012). Crystallization and preliminary X-ray analysis of *S*-ribosylhomocysteinase from *Streptococcus mutans*. *Acta Crystallographica Section F: Structural Biology and Crystallization Communications, 68*(2), 199–202.

Li, J., Wang, W., Wang, Y., & Zeng, A.-P. (2013). Two-dimensional gel-based proteomic of the caries causative bacterium *Streptococcus mutans* UA159 and insight into the inhibitory effect of carolacton. *Proteomics, 13*(23–24), 3470–3477.

Lin, Y., Shen, C., Zhao, J., Wang, C., Obara, M., Maung, A. T., Morita, M., Abdelaziz, M. N. S., Masuda, Y., Honjoh, K.-I., & Miyamoto, T. (2024). Antibacterial effect and mechanism of theaflavin against *Listeria monocytogenes* and its application on apple skins. *Journal of Food Science, 89*(10), 6653–6663.

Liu, C., Zhang, H., Peng, X., Blackledge, M.S., Furlani, R.E., Li, H., Su, Z., Melander, R. J., Melander, C., Michalek, S., & Wu, H. (2023). Small molecule attenuates bacterial virulence by targeting conserved response regulator. MBio, 14(3), e00137-23.

Lobo, C. I. V., Lopes, A. C. U. D. A., & Klein, M. I. (2021). Compounds with distinct targets present diverse antimicrobial and antibiofilm efficacy against *Candida albicans* and *Streptococcus mutans*, and combinations of compounds potentiate their effect. *Journal of Fungi, 7*(5), 340.

Maklennan, A., Borg-Bartolo, R., Wierichs, R. J., Esteves-Oliveira, M., & Campus, G. (2024). A systematic review and meta-analysis on early-childhood-caries global data. BMC Oral Health, 24(1), 835.

Mao, Y., Liu, P., Chen, H., Wang, Y., Li, C., & Wang, Q. (2023). Baicalein Inhibits the *Staphylococcus aureus* Biofilm and the LuxS/AI-2 System in vitro. Infection and Drug Resistance, 2861-2882.

Matias Regis, W. F., Rocha, F. R., Lima, R. A., Costa, A. C., Duarte, S., Brilhante, R. S. N., & Rodrigues, L. K. A. (2025). The synergistic relationship between *Streptococcus mutans* and *Candida albicans* in dental caries: Emerging therapeutic targets in biofilm modulation. *Cureus, 17*(6), e86159.

Mazurel, D., Brandt, B. W., Boomsma, M., Crielaard, W., Lagerweij, M., Exterkate, R. A. M., & Deng, D. M. (2025). Streptococcus mutans and Caries: A Systematic Review and Meta-Analysis. *Journal of dental research*, *104*(6), 594-603.

McNeill, K., & Hamilton, I. R. (2004). Effect of acid stress on the physiology of biofilm cells of Streptococcus mutans. Microbiology, 150(3), 735-742.

McKernan, L. N. (2015). Using a simple Escherichia coli growth curve model to teach the scientific method. The American Biology Teacher, 77(5), 357-362.

Mishra, R., Nikam, A., Hiwarkar, J., Nandgude, T., Bayas, J., & Polshettiwar, S. (2024). Flavonoids as potential therapeutics in male reproductive disorders. Future Journal of Pharmaceutical Sciences, 10(1), 100.

Mogen, A. B., Chen, F., Ahn, S.-J., Burne, R. A., Wang, D., & Rice, K. C. (2015). Pluronics-formulated farnesol promotes efficient killing and demonstrates novel interactions with *Streptococcus mutans* biofilms. *PLoS ONE, 10*(7), e0133886.

Moo, C. L., Osman, M. A., Yang, S. K., Yap, W. S., Ismail, S., Lim, S. H. E., Chong, C. M., & Lai, K. S. (2021). Antimicrobial activity and mode of action of 1,8-cineol against carbapenemase-producing *Klebsiella pneumoniae*. *Scientific Reports, 11*(1), 1–13.

Moon, J., Seo, K., & Kwon, J. S. (2025). Novel two-stage expansion of Streptococcus mutans biofilm supports EPS-targeted prevention strategies for early childhood caries. npj Biofilms and Microbiomes, 11(1), 65.

Murtey, M. D., & Ramasamy, P. (2021). Life science sample preparations for scanning electron microscopy. Acta Microscopica, 30(2), 80-91.

Paglia, L. (2025). Early Childhood Caries: a Family-Centred Disease. European journal of paediatric dentistry, 26(2), 87.

Patel, N. S., Mehta, M., Fu, Y., Desai, V., Lala, H. S., Parikh, H., … & Thakor, U. B. (2025). A Review of Early Childhood Caries: Risk Factors, Management, and Policy Recommendations. Cureus, 17(5).

Pitts, N. B., Zero, D. T., Marsh, P. D., Ekstrand, K., Weintraub, J. A., Ramos-Gomez, F., Tagami, J., Twetman, S., Tsakos, G. & Ismail, A. (2017). Dental caries. Nature reviews Disease primers, 3(1), 1-16.

Prince, A., Roy, S., & McDonald, D. (2022). Exploration of the antimicrobial synergy between selected natural substances on Streptococcus mutans to identify candidates for the control of dental caries. Microbiology Spectrum, 10(3), e02357-21.

Quivey, R. G., Jr., Faustoferri, R. C., Santiago, B., Baker, J., Cross, B., & Xiao, J. (2016). Acid-adaptive responses of *Streptococcus mutans*, and mechanisms of integration with oxidative stress. In F. J. de Bruijn (Ed.), *Stress and environmental regulation of gene expression and adaptation in bacteria* (Vol. 2, pp. 897–910). Wiley-Blackwell.

Regis, W. F. M., Rocha, F. R., Lima, R. A., Panariello, B., Duarte, S., da Cunha Costa, A., ... & Costa Sr, A. D. C. (2025). Insights Into the Role of *Streptococcus mutans* and *Candida albicans* in Dental Biofilm Formation and Cariogenicity: A Literature Review. Cureus, 17(6).

Requena, R., Vargas, M., Chiralt, A. 2019. Study of the potential synergistic antibacterial activity of essential oil components using the thiazolyl blue tetrazolium bromide (MTT) assay. Lwt, 101, 183-190.

Robles-Gómez, L., Sáez-Espinosa, P., & Gómez-Torres, M. J. (2025). Field emission scanning electron microscopy (FE-SEM) as an approach for membrane surface mapping in cell biology. In *Methods in Molecular Biology* (Vol. 2897, pp. 435–444).

Rocha, F. R., Regis, W. F., Duarte, S., Muniz, F. W., & Rodrigues, L. K. (2020). Effect of bioactive compounds on the regulation of quorum sensing network-associated genes and virulence in *Streptococcus mutans*—A systematic review. Archives of Oral Biology, 119, 104893.

Rusali, R., Najwa Hamali, N., Muhammad Razi, F., Mustafa, N., Asilah Harun, N., & Azwani Mohd Shukri, N. (2019). Early childhood feeding practices and its association with early childhood caries. *Journal of Food and Nutrition Research*, *7*(11), 801-804.

Sanguansermsri, D., Sanguansermsri, P., Buaban, K., Kawaree, R., & Wongkattiya, N. (2024). Antimicrobial activity and time-kill kinetics of Boesenbergia rotunda essential oil and geraniol alcohol against oral bacterial pathogens. *Journal of Applied Pharmaceutical Science,* 14(2), 215-221.

Sara, Y., Gordo, B., Nadia, A., Kamel, M., MESSAOUDI, O., Mohammed, G., & Abdel Ilah, A. (2024). Exploring Teucrium aureo-candidum Essential Oil as a Promising Alternative to Triclosan for Targeting Enoyl-Acyl Carrier Protein Reductase: Chemical Composition, Antibacterial Activity, and Molecular Docking Study. Chemistry & Biodiversity, e202401945.

Sen, A. K., Sen, D. B., Zanwar, A. S., Balaraman, R., Shah, U., & Maheshwari, R. A. (2022). Catechins and theaflavins: An overview on therapeutic application. Journal of Natural Remedies, 22(3), 331–344.

Shamrin, T., Hossain, M. N., Jannat, T., Ahmed, B., Islam, S., & Rahman, M. A. (2025). Dental Caries-Microbiological Investigation in Patients Attending a Dental Clinic. Molecular Mechanism Research, 3(1), 8887.

Shi, Y.-H., Shen, J.-X., Tao, Y., Xia, Y.-L., Zhang, Z.-B., Fu, Y.-X., Zhang, K.-Q., & Liu, S.-Q. (2025). Dissecting the binding affinity of anti-SARS-CoV-2 compounds to human transmembrane protease, serine 2: A computational study. *International Journal of Molecular Sciences, 26*(2), Article 587.

Sinicropi, M. S., Iacopetta, D., Ceramella, J., Catalano, A., Mariconda, A., Pellegrino, M. & Aquaro, S. (2022). Triclosan: A small molecule with controversial roles. *Antibiotics*, *11*(6), 735.

Syal, K. (2017). Novel method for quantitative estimation of biofilms. *Current Microbiology, 74*(10), 1194–1199.

Vijayakumar, A., Sarveswari, H.B., Vasudevan, S., Shanmugam, K., Solomon, A.P., Neelakantan, P. Baicalein Inhibits *Streptococcus mutans* Biofilms and Dental Caries-Related Virulence Phenotypes. Antibiotics 2021, 10, 215.

Wang, S., Wang, Y., Wang, Y., Duan, Z., Ling, Z., Wu, W., Tong, S., Wang, H., & Deng, S. (2019). Theaflavin-3,3′-digallate suppresses biofilm formation, acid production, and acid tolerance in *Streptococcus mutans* by targeting virulence factors. *Frontiers in Microbiology, 10*, Article 1705.

Wang, S., Deng, S., & Wang, Y. (2024). Theaflavin-3, 3'-digallate effectively attenuates biofilm formation by *Enterococcus faecalis* via the targeting of specific quorum sensing pathways. Microbial Pathogenesis, 106739.

Wang, Y., Lee, S. M., & Dykes, G. A. (2013). Potential mechanisms for the effects of tea extracts on the attachment, biofilm formation and cell size of *Streptococcus mutans*. Biofouling, 29(3), 307-318.

Wang, Y., Li, C., Li, J., Ren, Z., Qiu, Y., Li, J., Decker, E. A., & Shan, Y. (2013). Theaflavin-3,3′-digallate inhibits *Streptococcus mutans* biofilm formation by suppressing gtf gene expression and disrupting cell membrane integrity. Food Chemistry, 138(2–3), 281–288.

Wang, Y., Samaranayake, L. P., & Dykes, G. A. (2022). Tea extracts inhibit the attachment of streptococci to oral/dental substrata by reducing hydrogen bonding energies. Biofouling, 38(1), 42-54.

Wint, W. Y., Miyanohara, M., Terada-Ito, C., Yamada, H., Ryo, K., & Murata, T. (2024). Effects of sucrose and farnesol on biofilm formation by *Streptococcus mutans* and *Candida albicans*. *Microorganisms, 12*(8), 1737.

Yoshida, T., Mori, K., Hatano, T., Okumura, T., Uehara, I., Komagoe, K., ... & Okuda, T. (1999). Studies on inhibition mechanism of autoxidation by tannins and flavonoids. *Chemical & Pharmaceutical Bulletin, 47*(10), 1341–1346.

Yu, L., Xu, X., Chua, W. Z., Feng, H., Ser, Z., Shao, K., Shi, J., Wang, Y., Li, Z., Sobota, R. M., & Sham, L. T. (2023). Structural basis of peptide secretion for quorum sensing by ComA. *Nature Communications, 14*(1), 7178.

Yue, J., Yang, H., Liu, S., Song, F., Guo, J., & Huang, C. (2018). Influence of naringenin on the biofilm formation of *Streptococcus mutans*. *Journal of Dentistry, 76*, 24–31.

Zhang, K., Lu, Z., & Guo, X. (2023). Advances in epidemiological status and pathogenesis of dental fluorosis. Frontiers in Cell and Developmental Biology, 11, 1168215.

Zheng, S., Hao, L., Zhang, L., Wang, K., Zheng, W., Wang, X., Zhou, X., Li, W., & Zhang, L. (2018). Tea polyphenols functionalized and reduced graphene oxide–ZnO composites for selective Pb^{2+} removal and enhanced antibacterial activity. *Journal of Biomedical Nanotechnology, 14*(7), 1263–1276.

APPENDICES

APPENDIX I

Result of the time killing assay over six hours

Time (Hour)	Log_{10} CFU/mL				
	Untreated	**1× MIC TF3-F**	**2× MIC TF3-F**	**1× MIC F**	**2× MIC F**
0	7.00 ± 0.00	7.00 ± 0.00	7.00 ± 0.00	7.00 ± 0.00	7.00 ± 0.00
2	7.35 ± 0.02	6.16 ± 0.59*	5.11 ± 0.26*	6.28 ± 0.43*	5.69 ± 0.09*
4	12.71 ± 0.41	5.60 ± 0.05*	4.94 ± 0.54*	5.87 ± 0.05*	5.64 ± 0.03*
6	12.10 ± 0.38	6.49 ± 0.40*	5.02 ± 0.37*	5.04 ± 0.49*	4.60 ± 0.02*

*$p < 0.05$ compared with untreated control at the same time point (one-way ANOVA followed by Tukey's post hoc test).

APPENDIX II

Result of membrane leakage assay against *S. mutans* at sublethal concentrations of F and TF3-F

Treatment	**$OD_{260\ nm}$**	**$OD_{280\ nm}$**
Untreated	2.462 ± 0.24	1.553 ± 0.77
½ MIC Farnesol	2.468 ± 0.24	1.546 ± 0.78
¼ MIC Farnesol	2.437 ± 0.26	1.247 ± 0.26
½ MIC TF3-F	3.037 ± 0.46	2.815 ± 0.55
¼ MIC TF3-F	2.790 ± 0.26	2.402 ± 0.72

APPENDIX III: PROOF OF PUBLICATION

MJFAS
Malaysian Journal of Fundamental and Applied Sciences

Abdullah *et al.* | Malaysian Journal of Fundamental and Applied Sciences, Vol. 21 (2025) 2314–2322

RESEARCH ARTICLE

A Molecular Docking Study on Anti-cariogenic Properties of Theaflavins against *Streptococcus mutans*

Muhammad Rizwan Shah Abdullah[a], Anis Fadhlina[a]*, Hassan Ibrahim Sheikh[b], Nur Iman Alia Baharuddin[a], Nur Hazirah Rosli[a], Khairul Bariyyah Abd Halim[c]

[a]Department of Fundamental Dental and Medical Sciences, Kulliyyah of Dentistry, International Islamic University Malaysia, 25200 Kuantan, Pahang, Malaysia; [b]Faculty of Fisheries and Food Science, Universiti Malaysia Terengganu, 21030 Kuala Nerus, Terengganu, Malaysia; [c]Department of Biotechnology, Kulliyyah of Science, International Islamic University Malaysia, 25200 Kuantan, Pahang, Malaysia

Abstract Early childhood caries (ECC) is an aggressive manifestation of dental decay, linked to high levels of *Streptococcus mutans* in dental plaque. In Malaysia, over 70% of children suffer from ECC, leading to premature tooth loss, malnutrition, and reduced quality of life. Common dental-care ingredients like triclosan and triclocarban pose health risks, necessitating safer alternatives. Theaflavins, bioactive compounds in black tea, show potential as natural antimicrobial agents. However, the precise molecular interactions of theaflavins with key virulence-associated proteins of *S. mutans* remain underexplored. This study aims to investigate the antibacterial mechanisms of theaflavins against *S. mutans* using in-silico methods. PyRx was used to evaluate the binding affinities of four selected compounds, theaflavin (TF1), theaflavin-3-gallate (TF2A), theaflavin-3'-gallate (TF2B), and theaflavin-3,3'-digallate (TF3), against seven *S. mutans* proteins (PDB 4TQX: Sortase A, PDB 6CAM: Glucan binding protein, PDB 3QE5: Cell surface protein, PDB 3VX4: Quorum sensing, PDB 3AIC: Glucosyltransferase, PDB 2W3Z: Immune evasion, PDB 3CZC: Carbohydrate uptake). All the ligands were prepared and optimised using Avogadro-1.2 prior to the molecular docking. BIOVIA Discovery visualizer was used to observe the protein-ligand interactions. Findings indicated that theaflavins exhibit significant binding affinities to various *S. mutans* proteins. Among all tested compounds, TF3 demonstrated the strongest binding affinities and favourable hydrogen bonding, particularly against glucan binding protein and glucosyltransferase. These results suggest that TF3 may serve as a promising lead compound for developing natural anti-caries therapeutics targeting *S. mutans* virulence mechanisms.

Keywords: Theaflavins, early childhood caries, anti-cariogenic, *Streptococcus mutans*, molecular docking.

***For correspondence:**
anis_fadhlina@iium.edu.my

Received: 25 Sept. 2024
Accepted: 11 June 2025

© Copyright Abdullah. This article is distributed under the terms of the Creative Commons Attribution License, which permits unrestricted use and redistribution provided that the original author and source are credited.

Introduction

Early childhood caries (ECC) is characterized by the presence of one or more decaying, missing, or filled tooth surfaces in any primary tooth in a child aged 71 months or less. *Streptococcus mutans* is widely known for its established role in caries aetiology. This oral health issue is particularly significant in underprivileged communities, both in developing and industrialized countries, where malnutrition is prevalent [1]. Despite advances in dental education and oral hygiene awareness, dental caries remains a serious public health challenge, with current global research indicating an increase in caries prevalence [2].

e-ISSN 2289-599X | DOI: https://doi.org/10.11113/mjfas.v21n4.3890

APPENDIX IV: PROOF OF ATTENDING CONFERENCES AS PRESENTER IN IIUM POSTGRADUATE COLLOQUIUM 2025

APPENDIX V: PROOF OF ATTENDING CONFERENCES AS PRESENTER IN 14TH DENTAL STUDENTS' SCIENTIFIC CONFERENCE